TÉCNICO LISBOA

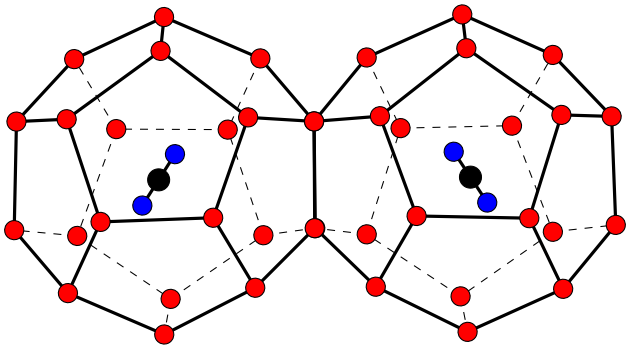

Feasibility analysis of CO_2 clathrate production for CO_2 sequestration and transport

Carmine Piparo

Thesis to obtain the Master of Science Degree in

Energy Engineering and Management

Supervisors: Prof. Maria Filipa Gomes Ribeiro
Prof. Vítor Manuel Geraldes Fernandes

Examination Committee

Chairperson: Prof. Francisco Manuel da Silva Lemos
Supervisor: Prof. Vítor Manuel Geraldes Fernandes
Member of the Committee: Prof. Carla Isabel Costa Pinheiro

June 2018

Dedicated to my family

Acknowledgments

Thanking everyone is no easy task, but i will try to do my best.

Firstly I would like to thank my supervisors, Professor Vitor Geraldes and Professor Filipa Ribeiro, for the useful hints and suggestions they gave me during the months of writing, despite my long absence.

I would also like to express my gratitude to Prof. Duarte de Mesquita e Sousa, for being the best programme coordinator ever and for his excellent support and advices at Instituto Superior Técnico and around Lisbon.

Many thanks go to InnoEnergy, for the chance of spending two years studying, travelling and working on projects all around Europe, with a special mention to Marta Abrantes and Diana Vittorino, always smiling and available in case of doubts.

More goes to all my friends, the old and the new ones, for all the encouragement and experience matured together over these past years. A special mention goes to all the SELECT family, you are amazing.

A very special mention goes to Giovanni Raffaele, Donato Colantuono and Marco di Ioia who not only supported and encouraged me but also put up with me for many years.

An exceptional acknowledgement goes to my brother, whose support was extremely important in hard times...but also in good times. I love you and I always will.

Finally, I would like to thank my whole family for their continued support, understanding and patience throughout my entire life. Nothing of this could have happened without their help, especially thanks to my parents whose love does not know any borders.

#ENVIRONOMICAL

Resumo

No último século, é de conhecimento geral que a concentração média de dióxido de carbono (CO_2) na atmosfera tem aumentado significativamente. Na última década, este assunto tornou-se mais relevante devido à taxa média de crescimento de 2 ppm/ano. Para fazer face a este crescimento, a abordagem mais promissora nas estratégias de redução de CO_2 é o Carbon Capture and Storage (CCS). Neste enquadramento, esta dissertação centra o seu enfoque nas tecnologias de pós-combustão, nas quais o CO_2 é separado dos gases de combustão, analisando diferentes métodos de separação e explorando a oportunidade de usar hidratos de gás, também conhecidos como clatratos, como processo alternativo de captura e armazenamento. Os clatratos são compostos cristalinos nos quais pequenas moléculas são capturadas por uma estrutura hospedeira de moléculas de água. Devido á sua elevada capacidade de armazenamento de gás, a separação baseada em clatratos pode ser uma alternativa às tecnologias de separação existentes e, ao adotar a água como meio de separação, é considerada como mais simples e amiga do ambiente. As tecnologias de captura de CO_2 penalizam fortemente a eficiência e custo de funcionamento das centrais de produção de energia. Neste contexto, o processo de hidratos é modelado por meio de um software de simulação, ASPEN-Plus, para avaliar os custos energéticos e de capital relacionados. Uma comparação entre uma separação baseada em MEA (Monoetanolamine) e o sistema de clatrato e THF (Tetrahydrofuran) é estudada para uma central a carvão supercrítico de 900 MW. Os resultados revelam que, para a separação baseada em MEA e em hidrados respectivamente, 37% e 39% da potência da central é necessária para reduzir as emissões de CO_2 até 90%. Apesar de terem um grande potencial, ao resultado anterior acresce ainda que, ao preço de mercado atual de eletricidade e de CO_2, nas condições tecnológicas e económicas analisadas os sistemas de captura de CO_2 ainda não são rentáveis.

Palavras-chave: CCS, CO_2, hidratos de gas, clatratos, ASPEN-Plus

Abstract

It is common knowledge that the observed mean carbon dioxide (CO_2) concentration in the atmosphere has been increasing significantly over the past century. The last decade attracted particular attention because of an average growth rate of 2 ppm/year. The most promising approach in the CO_2 abatement strategies is CCS (Carbon Capture and Storage). This work focuses on post-combustion technologies in which CO_2 is separated from flue gases. It briefly analyses different separation methods and explores the opportunity to use gas hydrates, also known as clathrates, as an alternative capture process and storage medium. Clathrates are crystalline compounds in which small molecules are caged in a host framework of water molecules. Due to its high gas storage capabilities, clathrate-based separation could be an alternative to the existing separation technologies and, by adopting water as a separation medium, it is considered simple and environment-friendly. CO_2 capture technologies add high energy penalties to power plants, therefore the hydrate process is modelled through a simulation software, ASPEN-Plus, to assess the related energetic and capital costs. A comparison between a MEA-based separation and the designed THF-clathrate system for a supercritical 900MW coal power plant reveals that, for the MEA-based and hydrate-based systems respectively, 37% and 39% of the net power output is needed to cut up to 90% of the CO_2 emissions. The results show that, at the current EU average CO_2 and electricity market price, the analysed techno-economic conditions deem CO_2 capture systems unprofitable, despite the great potential.

Keywords: CCS, CO_2, gas-hydrates, clathrates, ASPEN-Plus

Contents

Acknowledgments v
Resumo vii
Abstract ix
List of Tables xiii
List of Figures xv
Nomenclature xvii

1 Introduction **1**
1.1 Motivation 2
1.2 Overview 2
1.3 Objectives 3
1.4 Thesis Outline 3

2 Literature Review **5**
2.1 CO_2 Capture Systems 5
2.1.1 Absorption 7
2.1.2 Adsorption 11
2.1.3 Membrane Separation 13
2.1.4 Hydrate Separation 14
2.1.5 Cryogenic Distillation 18
2.1.6 Mineral Carbonation 19
2.2 Clathrate-based separation 19
2.2.1 Process Description 19
2.3 Summary of key findings 23

3 Process Model **25**
3.1 Process Simulation Tool: ASPEN-Plus 25
3.2 Methodology 25
3.2.1 ELECNRTL model 26
3.2.2 ASPEN-Plus Simulation of Clathrate Formation 28
3.2.3 Data used 28
3.2.4 Plant Layout 30

3.2.5 Equipment Analysis . . . 32
3.3 Model Outputs . . . 35

4 Post-combustion amine-based CO_2 absorption **37**
4.1 Amine-based absorption . . . 37
4.1.1 Choice of the sorbent . . . 37
4.1.2 Limitations of the MEA process . . . 38
4.2 Process Description . . . 39
4.2.1 Equipment Analysis . . . 40
4.3 Outputs . . . 41

5 Results **43**
5.1 Energy and cost Comparison . . . 43

6 Conclusions **49**
6.1 Future Work . . . 50

Bibliography **51**

A Appendix A **57**

List of Tables

2.1 Advantages and disadvantages of CO_2 capture choices 6
2.2 Summary of some characteristics of the three crystal hydrate structures 16
2.3 Ratio of molecular diameter to cavity diameter for few gaseous guest molecules 17

3.1 Flue gas composition 29
3.2 Design general parameters 30
3.3 Reaction parameters with THF 5% molar 30
3.4 Equipment flows main parameters 33
3.5 Model Output 36
3.6 Initial cost estimation 36

4.1 Power and energy needs 41

5.1 Energy comparison main outcomes 43
5.2 Basic cost comparison outputs considering fixed carbon and electricity market prices . . . 44
5.3 Hydrate separation system costs 44
5.4 Alternative scenario cost outputs 46

List of Figures

1.1 Averaged CO_2 from four GMD Baseline observatories: Barrow (Alaska), Mauna Loa (Hawaii), American Samoa, and South Pole (Antarctica). 1

2.1 Carbamate 7
2.2 Piperazine 9
2.3 Membrane configurations: Cross flow (a) and dead-end flow (b) 13
2.4 P–T diagram showing solubility isopleths of $CO_{2(aq)}$ between 0.25 and 4 mol% 15
2.5 Crystal structures of gas hydrates 16
2.6 Tetrahydrofuran, THF 17
2.7 Tetra-n-butyl ammonium bromide, TBAB 17
2.8 Representative solubility–supersolubility diagramn 20
2.9 Surface free energy (ΔG_s) and bulk free energy (ΔG_v) as functions of cluster size 21

3.1 Incipient hydrate formation equilibrium. 16.9% CO_2, 83.1% N_2 29
3.2 Process flow scheme for hydrate-based CO_2 capture from flue gas 31

4.1 Process flow scheme for amine-based CO_2 capture from flue gas 39

5.1 NPV chart with a payback period of 25 years 45
5.2 NPV chart with a payback period of 10 years 45
5.3 NPV chart with a payback period of 5 years 46
5.4 NPV chart with a payback period of 21 years 47
5.5 NPV chart in case of CO_2 sales at 5€$/ton$ 47

Nomenclature

APC	Aspen Custom Modeller
APP	Aspen Physical Property
CCS	Carbon Capture and Storage
COP	Conference Of the Parties
DEA	Dietanolamine
ECBM	Enhanced Coal Bed Methane
ELECNRTL	Electrolytes Non-Random Two-Liquid
EOR	Enhanced Oil Recovery
GHG	Green House Gas
ICE	Integrated Cost Estimation
IGCC	Integrated Gasification Cycle
LLE	Liquid-Liquid Equilibrium
MDEA	Methyl-dietanolamine
MEA	Monoetanolamine
NIST	National Institute of Standards and Technology
NPV	Net Present Value
NRTL	Non-Random Two-Liquid
NRTL-RK	Non-Random Two-Liquid Redlich-Kwong
O&M	Operation & Maintenance
PEI	Polyethyleneimine
PSA	Pressure Swing Adsorption
TBAB	Tetra-n-butyl ammonium bromide
THF	Tetrahydrofuran
TSA	Temperature Swing Adsorption
VLE	Vapour-Liquid Equilibrium

Absorption

C_{CO_2} Dissolved concentration of CO_2

K_{CO_2} CO_2 solubility

K_{HCO_2} CO_2 Henry's law constant

P_{CO_2} CO_2 partial pressure

Adsorption

α Probability of a particle to stick to the surface after a single collision

β Rate constant for desorption

Δ Working capacity

ΔH_{abs} Heat of adsorption

$\ni$ Frequency of collisions

θ Fraction of occupied adsorption sites

θ_{eq} Equilibrium coverage

K Boltzmann constant

m Mass

m_s Mass of sorbent

P Pressure

Q Activation energy for desorption

q Sorbate production rate

R Universal Gas constant

T Temperature

t_c Adsorption cycle duration

Cryogenic Distilation

α_{ij} Relative volatility of a binary mixture

C_L Concentration of the substance in the liquid phase

C_V Concentration of the substance in the vapour phase

K Vapour-liquid distribution ratio

Clathrate-based Separation

Δc Concentration difference (Supersaturation condition)

ΔG_s Gibbs free energy of the interface

ΔG_v Gibbs free energy of the bulk

Δg_v Free energy change per unit volume

ΔG	Gibbs free energy
$\dot{m}_H$	Total hydrate mass flow
$\dot{m}_H$	Total mass flow
$\dot{n}_H$	Total amount of hydrate formed
$\dot{n}_{sys}$	Hydrates remaining in the system
$\dot{n}_{tot}$	Total amount of hydrate present
η	Hydrate occupancy
ρ_H	Hydrate density
ρ_{sol}	Solution density
ρ_s	Slurry density
σ	Surface tension at the hydrate-liquid interface
f_{CO_2}	CO_2 fugacity in the liquid phase
f_H	CO_2 fugacity in the hydrate phase phase
MW_H	Hydrate molecular weight
P^{int}	Hydrate interface pressure at equilibrium (vapour-liquid)
R	Universal gas constant
r_c	Critical radius
S	CO_2 moles caged
T	Hydrate temperature at equilibrium
T_{exp}	Experimental temperature
$V_{mol,H}$	Hydrate molar volume
w_H	Hydrate mass fraction in the slurry
x^{int}	CO_2 equilibrium concentration
x^{tb}	CO_2 concentration at turbidity
x_H	Hydrate mass fraction
z	Gas Compressibility

ELECNRTL model

μ_k^{∞}	Aqueous infinite diluition potential
$\mu_s^{*,l}$	Non-water solvent potential
$\mu_w^{*,ig}$	Ideal water thermodynamic potential
μ_w^{*}	Water thermodynamic potential
$C_{p,k}^{\infty,aq}$	Aqueous infinite dilution heat capacity

$G_k^{\infty,aq}$	Aqueous infinite dilution Gibbs free energy
$G_m^{*,E}$	Molar Gibbs free energy
G_m^*	Molar excess Gibbs free energy
$H_{k,w}$	Solubility constant
H_k^∞	Infinite diluition enthalpy
H_k^∞	Infinite diluition entropy
p	Pressure
p^{ref}	Reference pressure
P_{ci}	Critical Pressure
R	Universal gas constant
T	Temperature
T_{ci}	Critical Temperature
V_m	Molar Volume
x_i	Molar fraction of the component i
x_j	Molar fraction of the component j
x_k	Molar fraction of the component k
x_s	Molar fraction of the non-water solvent
x_w	Molar fraction of water
y_i	Activity coefficient

Chapter 1

Introduction

Nowadays, it is common knowledge that the observed carbon dioxide (CO_2) concentration in the atmosphere has been increasing significantly over the past century. Data show the passage from about 280 ppm in the pre-industrial era to an average concentration greater than 400 ppm. The last decade attracted particular attention because of an average growth rate of 2 ppm/year (see figure 1.1)[1]. The IPCC report on Climate Change 2014 highlights that human influence on the climate system "is ex-

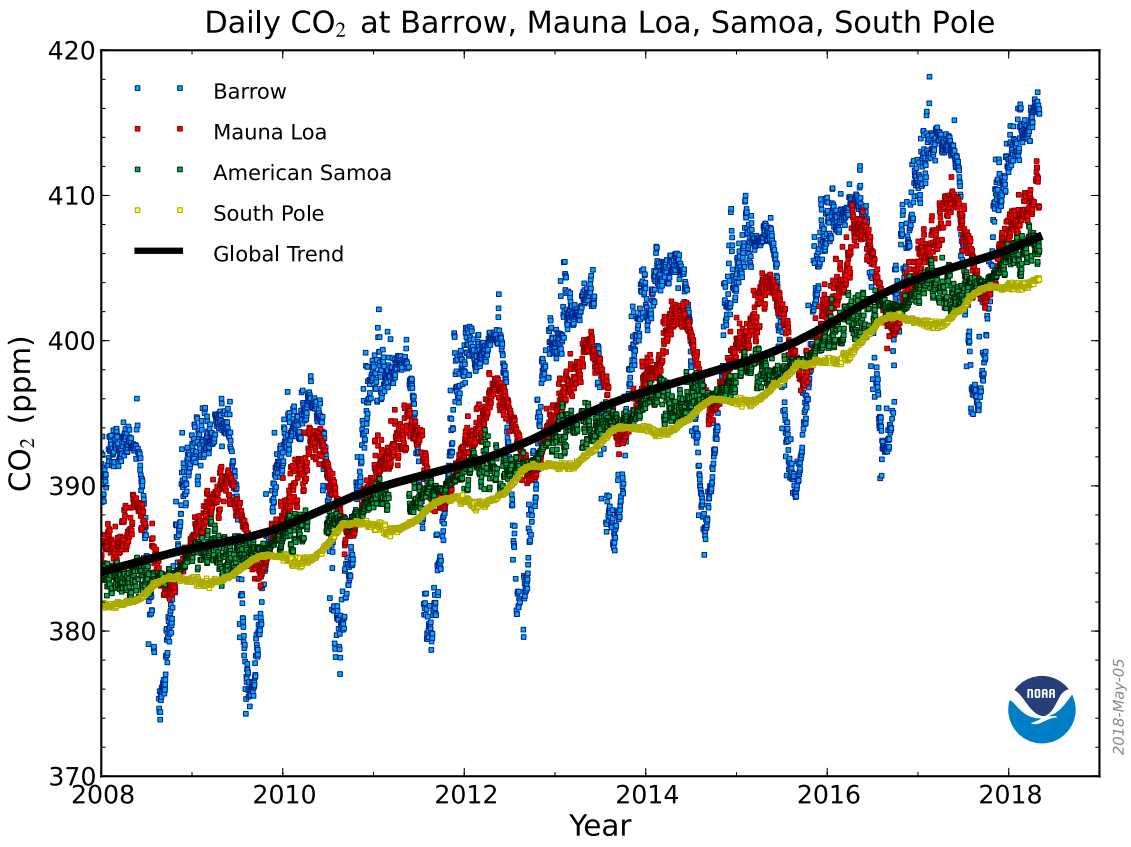

Figure 1.1: Averaged CO_2 from four GMD Baseline observatories: Barrow (Alaska), Mauna Loa (Hawaii), American Samoa, and South Pole (Antarctica).
[1]

tremely likely to have been the dominant cause of the observed warming since the mid-20th century"[2]. In recent years, though, governments pushed towards a progressive promotion of sustainable development in the energy sector to fight climate change and face the related environmental issues. Although this paradigm shift is globally occurring, the energy sector remains the largest source emitting Green House Gas (GHG). CO_2 emissions account for the largest share, about 60% of the global emissions, followed by smaller amount of CH_4 and N_2O from agriculture, domestic livestock, rice cultivation and industrial processes not related to energy. These increased levels of emissions are mainly due to the growing demand for energy coming from global economic growth and development. Emissions in developing countries continued to increase driven by the use of coal and natural gas while emissions in developed countries decreased along the small reduction in coal and natural gas usage. 32.4 $GtCO_2$ emitted from fuel combustion alone were registered at the end of 2014[3]. A decisive turning point was encountered in 2015 during the 21st Conference of the Parties (COP21) in Paris, which resulted in the first international climate agreement that extended mitigation obligations to all countries, developed and developing. This made imperative to diminish the amount of CO_2 emitted to the atmosphere. In order to significantly reduce emissions, a combined effort is needed in the following areas: improving energy efficiency (promotes energy conservation), increase the usage of low carbon fuels, integrate more renewable energy sources, reforestation and Carbon Capture and Storage (CCS). The most promising approach in the abatement strategies is CCS because it would allow to reduce emissions not only in the energy sector (especially the fossil fuel based) but also in industrial sectors such as iron and steel manufacturing, petrochemical, and cement industry. As stated in the IEA report on CCS 2015: "CCS could deliver 13% of the cumulative emissions reductions needed by 2050 to limit the global increase in temperature to 2°C"[4]. This thesis work discuss CCS with focus on the CO_2 separation technologies.

1.1 Motivation

This work explores the opportunity to use gas hydrates, also known as clathrates, as an alternative capture process and storage medium. Due to its exceptionally high gas storage capabilities, clathrate-based separation could be an alternative to the existing separation technologies and, by adopting water as a separation medium it is considered simple and environment-friendly. Using water as a recyclable solvent means that there are significantly fewer hazards compared to other solvents and, in case of contamination, water can be disposed and replaced at significantly lower expense compared to other solvents. Additionally, this technology has the potential to recover more than 90 % of the CO_2 in the gas stream.

1.2 Overview

Capture technologies can mainly be divided in three categories, namely pre-combustion, post-combustion and oxy-fuel combustion. In pre-combustion technologies the primary fuel is processed in a reactor to produce CO_2 and H_2 to be used as fuel, while oxy-fuel combustion substitute air with oxygen in the

combustion process, generating mainly H_2O and CO_2. This thesis work focuses on post-combustion technologies, in which CO_2 is separated from flue gas (exhaust gas). At this time, several CO_2 separation processes are being tested, such as membrane or cryogenic separation, solvent absorption and solid adsorption[5]. Despite their advanced stage of development, these CCS processes present several drawbacks for practical applications: high cost of materials, high energy requirements, high solvent toxicity and high corrosion potential. Currently, the leading technology is based on solvent scrubbing with amine-based solvents, mainly monoethanolamine (MEA) or solvent based on sterically hindered amines (KS-1). These capture systems are a proven technology commercially available today, but suffer a high-energy penalty: substantial amount of heat or steam are required for sorbent regeneration, impacting the overall efficiency of the power plant[5]. This work explores the opportunity to use gas hydrates, also known as clathrates, as an alternative capture process and storage medium. Clathrates are crystalline compounds in which small molecules are caged in a host framework of water molecules. Due to its exceptionally high gas storage capabilities, clathrate-based separation could be an alternative to the existing separation technologies and, by adopting water as a separation medium it is considered simple and environment-friendly.

1.3 Objectives

It is well known that CO_2 capture technologies add high energy penalties to power plants and this translates into higher economic costs. The objective of this thesis is to evaluate the feasibility of producing CO_2 clathrate for CO_2 sequestration and transport. A comparison between amine-based separation technology and clathrate-base systems will hopefully give the means to understand the feasibility of the hydrate separation technology.

1.4 Thesis Outline

This works counts 6 chapters. Chapter 1 introduces the whole work. Chapter 2 gives an overview of the theoretical framework related to CO_2 capture processes and technologies. It briefly analyses different separation methods focusing on post-combustion, amine-based and clathrate process technologies. Chapter 3 presents the process modelled, giving an overview of the simulation tool, ASPEN-Plus. It describes the adopted methodology and the plant layout based on an existing $900MW$ coal power plant. Chapter 4 describes the amine absorption process and reports the results as obtained by a specific analysis on the mentioned $900MW$ coal power plant, for the energetic comparison with the hydrate-based methods. Results are summarised in chapter 5 with an energetic comparison between the analysed processes and an initial economic analysis. Finally, chapter 6 draws conclusions and proposes ideas for future works.

Chapter 2

Literature Review

This chapter gives an overview of the theoretical framework related to CO_2 capture processes and technologies. It briefly analyses different separation methods focusing on post-combustion, amine-based and clathrate process technologies.

2.1 CO_2 Capture Systems

CO_2 capture processes are mainly divided in three categories, namely pre-combustion, post-combustion and oxy-fuel combustion.

Pre-combustion In this process, the CO_2 sequestration happens before the combustion phase and counts three main phases:

- Syngas (CO + H_2) formation through fuel gasification (coal) or gas reforming (CH_4)

$$\text{Coal} \xrightarrow{\text{gasification}} \text{CO} + \text{H}_2 \tag{2.1}$$

$$\text{CH}_4 \xrightarrow{\text{reform}} \text{CO} + \text{H}_2 \tag{2.2}$$

- Increase the amount of H_2 formed and convert CO into CO_2 with the water gas shift reaction

$$\text{CO} + \text{H}_2\text{O} \xrightarrow{\text{water-gas-shift}} \text{CO}_2 + \text{H}_2 \tag{2.3}$$

- CO_2 capture with the possibility of using different separation processes which will be discussed further on.

In the pre-combustion process, the CO_2 separation is facilitated because of its high concentration in the fuel gas mixture and because of a great difference in molecular weight and diameter with H_2 rather than with N_2. Afterwards, CO_2 is sent to the compression unit, therefore the total energy required for separation and compression is lower when compared with oxy-fuel or post-combustion. Hydrogen is

then burned with air, generally used as input for combined cycle for electricity production, obtaining mainly N_2 and water vapour in the exhaust gas. Excluding storage and transport, studies show that applying pre-combustion capture technologies to Integrated Gasification Combined Cycle (IGCC) power plants result in efficiency losses varying from 7 to 10% if compared to a power plant without CCS[6].

Oxy-fuel combustion Oxygen (purity up to 97%) substitute air in the combustion phase, reducing greatly the amount of N_2 and thermal NO_x formation in the exhaust gasses. This substitution results in an exhaust gas final composition of, mainly, CO_2, H_2O, SO_2 and particulate. After processing the gas in order to condense water, and purify it through desulphurization and electrostatic precipitation, the remaining composition is high on CO_2 (up to 99%) and can then be compressed, transported and stored. This process consumes large amounts of oxygen and the high SO_2 concentration may worsen the corrosion problems. These aspects, coupled with an energy penalty that can surpass 7% if compared to a power plant without CCS, increase a lot the overall cost of the process[7].

Post-combustion Due to the removal of CO_2 taking place after the combustion phase, this process results to be preferred for retrofitting existing power plants. However, normally the amount of CO_2 in the flue gas of existing power plants is relatively low (7-14% for coal-fired and 4% for gas-fired), this brings a major challenge for the CO_2 capture process in exam: the energy penalty and associated costs for the capture unit to reach the concentration of CO_2 needed (above 95%) for transport and storage are elevated[7]. Due mainly to the commercial deployment and development of the technology in the industrial sector and due to the chance of virtually retrofit any existing power plant, the choice of this analysis fell on the post-combustion option. Table 2.1 summarise advantages and disadvantages of these capture options.

Table 2.1: Advantages and disadvantages of CO_2 capture choices

Advantages and disadvantages of CO_2 capture choices		
Capture choices	Advantages	Disadvantages
Pre-Combustion	Low energy required for CO_2 separation and compression	The H_2 rich gas can give temperature and efficiency issues
Oxy-fuel combustion	Mature air separation technology (O_2 purity up to 97%)	Large consumption of O_2 High SO_2 concentration worsen the corrosion problem
Post-combustion	Fully commercially developed and deployed technology Chance to retrofit existing plants	High energy penalty for solvent regeneration High capital and operation costs

Six main technologies are currently in use or being developed: chemical or physical absorption, chemical or physical adsorption, membrane and hydrate separation, mineral carbonation and cryogenic distillation. Sections from 2.1.1 to 2.1.6 briefly analyse these fundamental technologies.

2.1.1 Absorption

Objective of this process is the removal of one or more component from a gas stream using a liquid sorbent, mainly adopted to remove acid gases such as CO_2 or H_2S, at high partial pressures. The target molecules enter the sorbent bulk and form a solution. When aiming at CO_2 removal at low partial pressure, this method uses amine or carbonate solutions as solvents, reaching CO_2 removal rate higher than 90%, depending on the amine-blend used, on the gas composition and on the system optimisation[8][9][10]. This is the most diffused CO_2 capture technology on an industrial scale and can be differentiated in physical and chemical absorption. If solvent and target component chemically react forming a chemical compound, the process is known as chemical absorption; if solute and target component are chemically inerts, the target component is physically absorbed by the solvent without any chemical reaction.

Chemical absorption

Amongst the most diffused chemical absorptions we can distinguish the amine-based, the carbonate-based, the aqueous-amine and the sodium hydroxide-based absorption. The reaction, forming a weakly bonded intermediate component between sorbent and target molecule is exothermic and facilitated at low temperature. The sorbent regeneration happens through a process called stripping that can take place at high temperature or by de-pressurisation. The selectivity of this separation method is high, making it very suitable for CO_2 separation.

Amine-based This method is currently the most used and mature for CO_2 separation. The separation process uses ammonia-derived (NH_3) organic compounds, the amines. Organic components, commonly indicated with the letter "R", substitute one or more ammonia hydrogen atoms and, in dependence on the number of substituents, they are labelled primary (R^1-NH_2), secondary (R^1R^2-NH) or tertiary ($R^1R^2R^3$-N) amines respectively. The most studied and commonly used sorbent is monoethanolamine (MEA) with R^1=CH_2CH_2OH, followed by diethanolamine (DEA) with R^1=R^2=CH_2CH_2OH and methyl-diethanolamine (MDEA) with R^1=R^2=CH_2CH_2OH and R^3=CH_3. Amines act like bases, they neutralise acid molecules like CO_2 by forming a weekly bonded component, the carbamate (shown in figure 2.1), and releasing heat. The energy released using MEA as sorbent is approximately 2.0 - 3.5 $MJ/kg CO_2$[6]. Equation

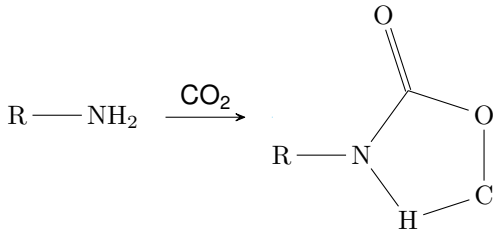

Figure 2.1: Carbamate

2.4 shows the reaction using a primary amine:

$$2\,R{-}NH_2 + CO_2 \longrightarrow R{-}NH_3^+ + R{-}NHCOO^- + \text{heat} \tag{2.4}$$

Although other two reactions contribute to the CO_2 absorption, base-catalysed hydration 2.5 and the formation of carbonic acid 2.6, the one driving the overall absorption rate is the reaction 2.4.

$$R{-}NH_2 + CO_2 + H_2O \longrightarrow R{-}NH_3^+ + HCO_3^- + \text{heat} \tag{2.5}$$

$$CO_2 + H_2O \longrightarrow H_2CO_3 \tag{2.6}$$

The carbamate-equivalent reaction for secondary amines is:

$$2\,R^1R^2{-}NH + CO_2 \longrightarrow R^1R^2{-}NH_2^+ + R^1R^2{-}NCOO^- + \text{heat} \tag{2.7}$$

For a tertiary amine the reaction leading the absorption rate is the base-catalysed hydration:

$$R^1R^2R^3{-}N + CO_2 + H_2O \longrightarrow R^1R^2R^3{-}NH^+ + HCO_3^- \tag{2.8}$$

As previously mentioned, the sorbent can be regenerated applying heat, therefore promoting the reverse reactions. Equations 2.9 and 2.10 show the reverse reactions for a primary amine, respectively, for the carbamate reaction 2.4 and for the base-catalysed hydration 2.5.

$$R{-}NH_3^+ + R{-}NHCOO^- + \text{heat} \longrightarrow 2\,R{-}NH_2 + CO_2 \tag{2.9}$$

$$R{-}NH_3^+ + HCO_3^- + \text{lessheat} \longrightarrow R{-}NH_2 + CO_2 + H_2O \tag{2.10}$$

The key factors for determining the optimal amine choice are a fast reaction rate, a low regeneration energy, and a high loading capacity. None of the amines alone excel in all the requirements, therefore the choice is not straightforward: the reaction rate is greater for primary amines while for regeneration energy and loading capacity the choice falls on tertiary (followed by secondary and primary). Moreover, in the presence of oxygen, amines are susceptible to degradation, known as oxidative deamination. Primary amine are more susceptible to this oxidation and the consequence is the formation of side products like HCOOH (formic acid) and NH_3. One of the current trend is to opt for blended amine solvents composed of a mix of primary, secondary, and tertiary amines, combining their respective strengths[11][12]. The amine-based separation system is analysed more in detail in chapter 4.

Carbonate-based This process is based on the natural phenomena of carbonate rocks dissolution (equation 2.12) as a consequence of the reaction between rain and CO_2 which results in carbonic acid formation, as shown in equation 2.11. In the carbonate-based system, flue gases pass through a reactor in which a continuous flow of water wets a bed of crushed limestone. The initial idea of adopting this method does not take into account the solvent regeneration but the disposition of the bicarbonate-rich product into the ocean.

$$H_2O + CO_2 \longrightarrow H_2CO_3 \tag{2.11}$$

$$CaCO_3 + H_2CO_3 \longrightarrow Ca^{2+} + 2\,HCO_3^- \tag{2.12}$$

It exists an alternative process that uses regenerable aqueous carbonate solutions like potassium carbonate (K_2CO_3) that, despite having lower rates of reaction for low CO_2 partial pressure (which is the case of flue gas), require lower desorption energy if compared to amine-based reactions (0.9 to 1.6 $MJ/kgCO_2$ instead of $\sim$3 $MJ/kgCO_2$)[6]. This process is based on a two stage reaction, shown in equations 2.13 and 2.14.

$$K_2CO_3 + H_2O \longrightarrow KOH + KHCO_3 \tag{2.13}$$

$$KOH + CO_2 \longrightarrow KHCO_3 \tag{2.14}$$

In order to increase the solvent absorption rate and capacity, a cyclohexane ring with amine functional groups, called Piperazine (figure 2.2), is used. Equations 2.15, 2.16 and 2.17 show the enhanced

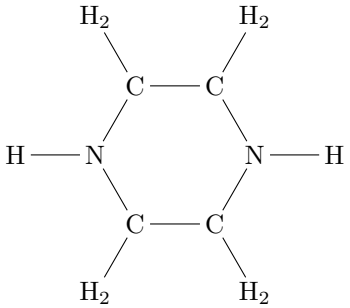

Figure 2.2: Piperazine

reaction process which requires significantly less heat for solvent regeneration compared to the MEA process.

$$KHCO_3 \longrightarrow K^+ + HCO_3^- \tag{2.15}$$

$$PZ + HCO_3^- \longrightarrow PZCOO^- + H_2O \tag{2.16}$$

$$PZCOO^- + HCO_3^- \longrightarrow PZ(COO-)_2 + H_2O \tag{2.17}$$

Aqueous amine-based An aqueous solution of $(NH_4)_2CO_3$ (ammonium carbonate) reacts with CO_2 and H_2O to form NH_4HCO_3 (ammonium bicarbonate). The reaction is shown in the equation 2.18.

$$(NH_4)_2CO_3 + CO_2 + H_2O \longleftrightarrow 2\,NH_4HCO_3 \tag{2.18}$$

Key advantages of this process is the lower heat of reaction compared to the MEA process and the potential to be used in multi-component flue gas emission control (scrubbing of SO_2 and NO_2)[6].

Sodium hydroxide-based The use of sodium hydroxide in the CO_2 absorption process involves three key reactions shown in equations 2.19, 2.20 and 2.21, respectively, carbonic acid formation, bicarbonate and carbonate formation:

$$H_2O + CO_2 \longrightarrow H_2CO_3 \tag{2.19}$$

$$H_2CO_3 + NaOH \longrightarrow NaHCO_3 + H_2O \tag{2.20}$$

$$NaHCO_3 + NaOH \longrightarrow Na_2CO_3 + H_2O \tag{2.21}$$

By adjusting the pH of the reaction it is possible to control the proportion of carbonate and bicarbonate in the products. The addition of CaO (lime) to the carbonation process serves the purpose of solvent regeneration (equations 2.22 and 2.23): the calcium carbonate slurry obtained is heated up to drive off the water, then follows a calcination process at 900 ℃ (equation 2.24).

$$CaO + H_2O \longrightarrow Ca(OH)_2 \tag{2.22}$$

$$Ca(OH)_2 + Na_2CO_3 \longrightarrow 2\,NaOH + CaCO_3 \tag{2.23}$$

$$CaCO_3 + heat \longrightarrow CaO + CO_2 \tag{2.24}$$

This process uses inexpensive and abundantly available chemicals, but it requires significantly high energy for $CaCO_3$ recovery (15 GJ/ton of CO_2)[6].

Physical absorption

Instead of chemical reactions, in the physical absorption, acid gas absorption by a solvent is regulated by the vapour–liquid equilibrium of the mix via Henry's law: at a given temperature, the amount of dissolved gas in unit volume of a solvent is proportional to the partial pressure of the gas in equilibrium with the solvent. The solubility of a gas, in this case CO_2, (K_{CO_2}) is:

$$K_{CO_2} = C_{CO_2}/P_{CO_2} = 1/K_{HCO_2} \tag{2.25}$$

where
$C_{CO_2} =$ dissolved concentration of CO_2
$P_{CO_2} =$ CO_2 partial pressure
$K_{HCO_2} =$ CO_2 Henrsy's law constant

As can be seen in equation 2.25, the concentration of a solute in a solvent is proportional to its partial pressure above the solvent. Therefore, a high ratio $mol\,CO_2/mol\,solvent$ can be achieved for high pressure gas streams or with a high CO_2 content (or the combination). The most common solvents used in physical absorption of CO_2 are methanol (CH_3OH) in the Rectisol process (separation from natural gas), propylene carbonate ($C_4H_6O_3$) in the Fluor process and dimethyl ethers of polyethylene carbonate ($CH_3(CH_2CH_2O)_nCH_3$) in the process Selexol®. Generally, the solubility of CO_2 in CH_3OH rises steeply at reducing temperatures, obtaining optimal separation between –60 ℃ and –70 ℃. While operating at low temperature, high pressure, or both, raising temperature or lowering pressure will release solute due to the lowering of its solubility. The physical solvent regeneration can be achieved by an increase in temperature or by a pressure reduction. The advantage of physical sorbents is being chemically inert to the treated gas, avoiding the formation of heat-stable salts, problematic in chemical absorption processes[6].

2.1.2 Adsorption

In the adsorption process, unlike absorption, the sorbate remains on the sorbent surface instead of entering the bulk and forming a solution. A solid sorbent is used instead of a liquid one but, similarly to the absorption, binding the adsorbate proceeds either through chemical or physical adsorption. Key aspect of a good sorbent is the amount of adsorbate it can hold, ergo the selection criteria count extensive specific surface area, great selectivity and high regeneration ability. A diverse range of sorbents is currently available while others are under development for CO_2 separation, moreover, sorbents combinations can yield great adsorption efficiencies. Common choices are activated carbon, zeolites, molecular sieves, calcium oxides, hydrotalcites and lithium zirconate. Main advantages compared to liquid absorption include a wide range of operating temperatures, no liquid-waste and, generally, environmental-friendly solid wastes that do not present many problems of disposal. The technological development of this technology started with air purification applications and rapidly expanded in the past decades also thanks to the development of new sorbent materials. In order to reduce the total cost of capture, new sorbents for CO_2 capture are being developed exploiting residues from industrial and agricultural operations[7][6][13][14].

Physical adsorption

The Langmuir isotherm describes the physical adsorption process, derived from a basic equilibrium between adsorption and desorption. Equation 2.26 and equation 2.27 describe, respectively, the rate of adsorption and desorption:

$$A = \alpha\nu(1-\theta) \tag{2.26}$$

$$B = \beta\theta e^{-Q/RT} \tag{2.27}$$

Where
$\theta =$ Fraction of occupied adsorption sites
$\alpha =$ Probability of a particle to stick to the surface after a single collision
$\beta =$ Rate constant for desorption
$R =$ Universal gas constant
$Q =$ Activation energy for desorption

The activation energy (Q) is also equal to the heat of adsorption (-ΔH_{abs}). For a given mass m (kg) and pressure P (Pa), ν (s^{-1}) represent the frequency of collisions, described in equation 2.28 (kinetic theory of gases):

$$\nu = P/(2\pi mkT)^{1/2} \tag{2.28}$$

Where k ($^J/_K$) is the Boltzmann constant and T (K) the absolute temperature. At equilibrium we have:

$$\alpha\nu(1-\theta) = \beta\theta e^{-Q/RT} \tag{2.29}$$

which gives us the equilibrium coverage θ_{eq}:

$$\theta_{eq} = KP/(1+KP) \tag{2.30}$$

where

$$K = \alpha e^{Q/RT}/\beta(2\pi mkT)^{1/2} \tag{2.31}$$

The equilibrium surface coverage for a multicomponent system will result in:

$$\theta_{eq,i} = K - iP_i/(1+\sum_{j=1}^{n} K_i P_i) \tag{2.32}$$

Gases are mainly adsorbed swinging pressure (PSA) or temperature (TSA). These systems rely on the preferential adsorption of one of the gas component at a certain temperature and pressure, followed by desorption by either lowering the pressure (PSA) or by increasing the temperature (TSA). For a given mass of sorbent m_s in an adsorption cycle of duration t_c the sorbate-rich production rate (ideal conditions) is described in equation 2.33.

$$q = m_s \Delta / t_c \tag{2.33}$$

where Δ is called the working capacity and it is the differential adsorptive sorbent capacity between the initial and final condition of pressure and temperature[6]. TSA processes have longer duration cycles when compared to PSA due to the needed heating and cooling time which is longer that the PSA pressurisation and depressurisation time. In general, having short duration cycles is preferred because it would mean to reduce the needed sorbent, plant size and costs, while keeping high adsorptive capacity. PSA for CO_2 recovery is already a commercially available technology that yields efficiencies above 90%[15][16]. TSA is also a promising technology that, although has a longer regeneration time, yields CO_2 purity higher than 95%, with recovery higher than 80%[17].

Chemical adsorption

Few of the absorbents described in the chemical absorption section (2.1.1) can be also used in solid form. The most frequently used are metal oxides, sodium carbonate and solid amine.

Metal oxides In this process, CO_2 is captured through carbonation of metal oxides, mainly calcium, sodium and potassium oxide. Examples of carbonation reactions are shown in equations 2.34 and 2.35. These reactions can also proceed with a further carbonation and produce bicarbonates.

$$CaO_{(s)} + CO_{2(g)} \longleftrightarrow CaCO_{3s} \tag{2.34}$$

$$Na_2O_{(s)} + CO_{2(g)} \longleftrightarrow Na_2CO_{3s} \tag{2.35}$$

The choice of metal oxide sorbents is often driven by the high temperature necessary for the decarbonation (400-600 °C), which makes these sorbent well suited for flue gas and syngas treatments.

Sodium carbonate Sodium carbonate can be also used, at lower temperatures, to capture CO_2 through carbonisation. Sodium bicarbonate (Na_2HCO_3) or Wegscheinder's salt ($Na_2CO_3 \cdot 3\,NaHCO_3$) can be obtained as products, as shown in equations 2.36 and 2.37. These reactions are exothermic (Δ_{abs}=-136 $kJ/mol CO_2$) and occur between 60 and 70 °C. The reverse reactions regenerate the sorbent and occurs around 120 - 200 °C

$$Na_2CO_3 + CO_2 + H_2O \leftrightarrow 2\,NaHCO_3 \tag{2.36}$$

$$Na_2CO_3 + 0.6\,CO_2 + 0.6\,H_2O \leftrightarrow 0.4\,(Na_2CO_3 \cdot 3\,NaHCO_3) \tag{2.37}$$

Solid amines Solid amine sorbents are solids with high specific area and functional groups attached onto their surface. Example of possible solids are alumina, meso/microporous silica or polymer based materials. An interesting fact is that, since 1990, space shuttle life-support systems use polyethyleneimine (PEI) bonded to acrylic-based polymer beads for CO_2 capture, regenerating the sorbent through vacuum swing desorption[6].

2.1.3 Membrane Separation

Due to the constant advancement in technology, a wide variety of membranes systems are potentially applicable or currently being studied. A membrane system acts as a filter that, through a series of chemical or physical processes, separates a specific component from a gas mixture. Membranes are made of a composite polymer with a thin selective layer bonded to a thicker one, generally non-selective and low-cost, that physically supports the membrane. Figure 2.3 shows the two commonly used module flow schemes for membrane separation. Basically, the feed gas enters the module, permeate the membrane

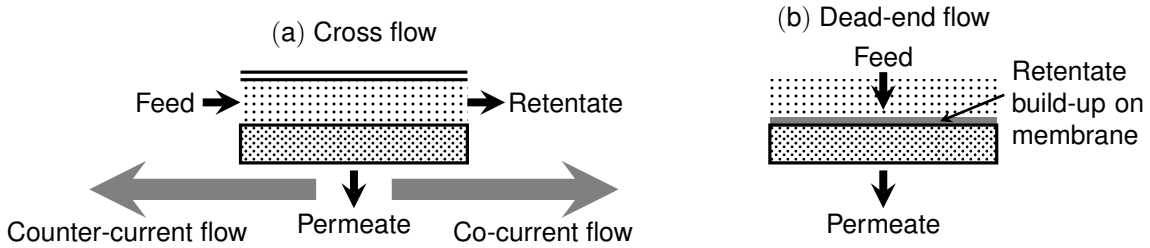

Figure 2.3: Membrane configurations: Cross flow (a) and dead-end flow (b)

and exits downstream. The retentate, (feed stream depleted of the permeate) can either exit the module (cross-flow scheme) or has to be continuously replenished (dead-end flow scheme). Membranes are classified as porous (pores equivalent diameter ranging from 0.001 to 0.1 μm) and non-porous (pores equivalent diameter smaller than 0.001 μm): membrane porosity is the key aspect determining the permeate transport mechanisms. Porous membranes are mainly used for micro-filtration (0.1 - 10 μm) and

ultra-filtration (0.001- 0.1 μm) while non-porous membranes focus on nano-filtration, reverse osmosis or molecular separation in the gas phase. In porous membranes, molecular transport depends primarily on the feed gas physical conditions of temperature and pressure and on the membrane pore size. On the macropore scale, gas flow is predominantly driven by viscous forces, while diffusion dominate the transfer when the pore size shrinks below the gaseous molecules mean free path. When approaching the molecular size (below 10 Å), surface interaction on the pore walls, better known as molecular sieving, dictates the flow transfer. For pore sizes smaller than (1 Å) a solution–diffusion mechanism dominates the transfer rather than molecular sieving[6]. Thanks to the advancement in this CO_2 separation technology, like the use of membrane contactors or through multiple stage membrane systems, it is currently possible to yield separation efficiencies above 90% with product purity up to 95%[18][19]. The major challenge in the application of this technology dwells within the flue gas physical conditions: membrane systems performance is heavily affected by the flue gas low pressure and CO_2 concentration ($\sim$15%) which translate into a low CO_2 permeation driving force. Therefore, to capture CO_2 from flue gas, specific requirements must be met, such as , high thermal and chemical stability, high CO_2 permeability, high CO_2/N_2 selectivity and acceptable costs. Because of these requirements, the only commercial available membrane type is polymer-based. The materials include polyamides, polycarbonates, polysulfone and cellulose acetate. In order to enhance the properties of polymeric membranes, a mixed-matrix structure is currently being analysed. The microstructure incorporate micro or nanoparticles of an inorganic material, in discrete phase, into a continuous polymeric matrix. This addition improves thermal and mechanical properties, especially in aggressive environments, and stabilizes the polymer membranes against chemicals and physical changes in the environment[20][21].

2.1.4 Hydrate Separation

This section will give a brief introduction on hydrates and the hydrate-based separation that is further developed in section 2.2. Hydrate-based separation is a relatively new technology for CO_2 capture: a flue gas mixture passes through chilled water at at high pressure (3 - 50 MPa) and low temperature (265 - 273 K); CO_2 molecules (and part of the other components) freeze with the water molecules and get trapped into solid crystalline cage-like structures, also known as clathrates. CO_2 and H_2O freeze together forming a slurry of ice crystals in liquid water, but not all the gas components are trapped in the ice crystals. The driving force for mass transfer is the CO_2 concentration difference between the bulk[1] liquid phase and the hydrate interface. Figure 2.4 shows the P–T diagram showing solubility isopleths of $CO_{2(aq)}$ between 0.25 and 4 mol%. The hydrates containing CO_2 molecules is separated from the other components for storage or transport purposes. CO_2 can be recovered by heating the slurry, therefore breaking the ice cages and releasing the gas molecules[22]. Gas hydrates are non-stoichiometric, solid compounds in which non-polar gas molecule are encaged in a frame of hydrogen bonded water molecules. These guest molecules, such as CH_4 and CO_2, are bound by van der Waals forces inside the polyhedral cavities of the hydrate structure[23][24]. Gas hydrates have been found to crystallise in three structure types: I, II, and H. Structures I and II crystallise within a cubic system while structure H follows

[1] The bulk concentration will increase at constant pressure and will not follow the concentration lines shown in figure 2.4

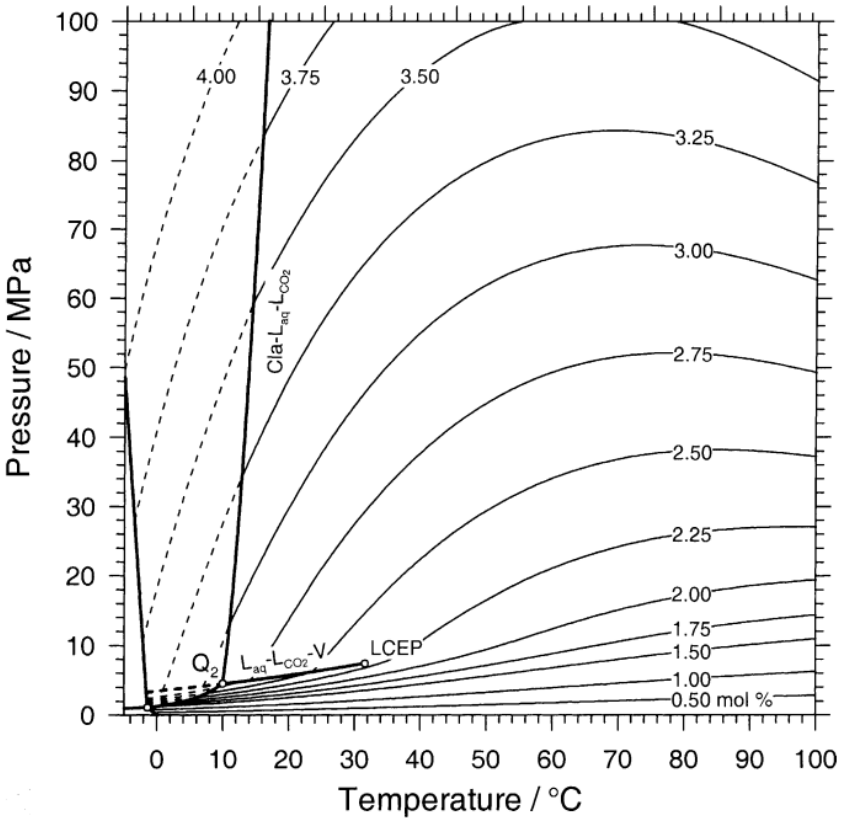

Figure 2.4: P–T diagram showing solubility isopleths of $CO_{2(aq)}$ between 0.25 and 4 mol%
Reproduced from Larryn W. Diamond, Nikolay N. Akinfiev, Solubility of CO2 in water from -1.5 to 100 °C and from 0.1 to 100 MPa: evaluation of literature data and thermodynamic modelling[22]

a hexagonal system. As shown in figure 2.5, the simplest and smallest cage is formed by twelve five-sided polyhedron (a.) while larger diameter cages can be formed by adding two (b.), four (c.) or eight (e.) hexagonal faces. Structure H has medium-size cavity formed by squared, pentagonal and hexagonal faces (d.). Thanks to the compact hydrate structure, high effective gas packing is possible. Table 2.2 summarises the hydrate structures characteristics[25]. A certain number of gas molecules are needed in order to stabilize the hydrate structure; occupied hydrate cages are function of the size ratio between guest molecule and host cavity. Structure I and II are most frequently observed during the clathrate crystallisation. For structure I and II, table 2.3 summarises the ratio $molecular\ diameter/cavity\ diameter$ for CO_2 and other guest molecules[26]. Structural stability of a hydrate composed of a single gas is reached for ratios of molecule to cage size of about 0.9; for ratios significantly lower than 0.9, the molecule will not stabilise enough the cage; when this ratio exceeds 1, the gas will not fit into the cavity; molecules larger than 7.5 Å will not fit into structure I and II cavities while molecules smaller than 3.5 Å will not stabilize the hydrate crystals. Generally, the formed structure depends on the largest molecule hosted[26]. Gas hydrates are identified with the chemical formula $nM \cdot H_2O$, with M referring to gas molecules and n referring to the number of gas molecules. Naturally, the formation of type I structure dominates and, with all the cavities occupied by a CO_2 guest molecule, the clathrate brute formula is:

$$8\,CO_2 \cdot 46\,H_2O \tag{2.38}$$

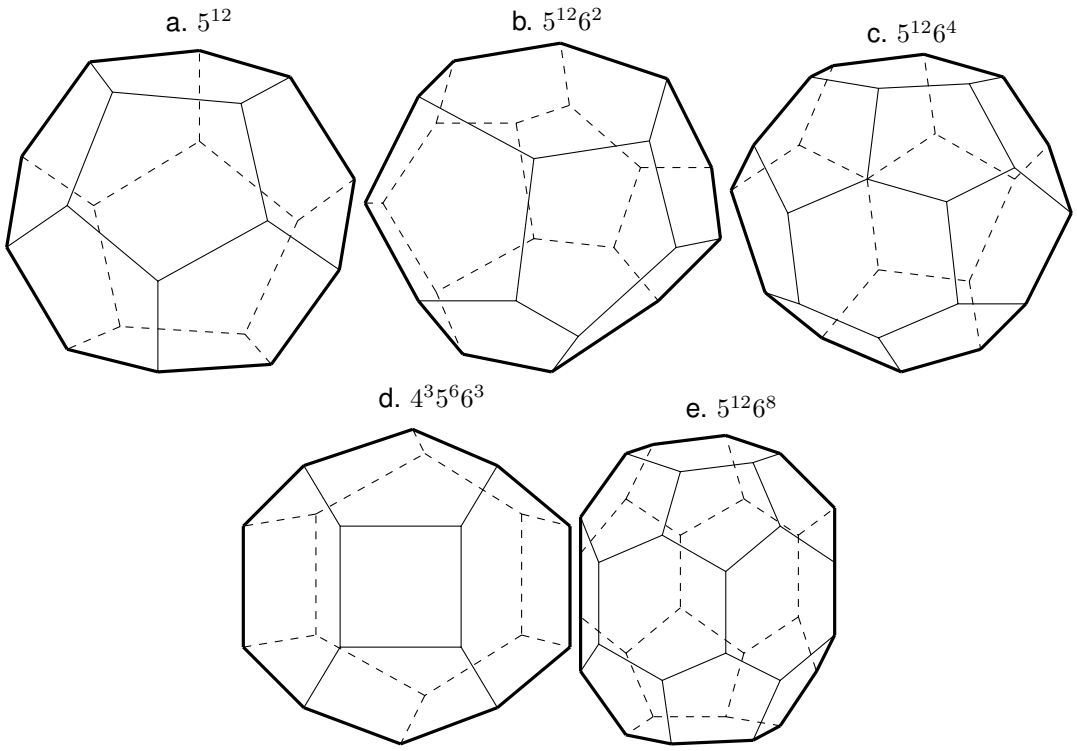

Figure 2.5: Crystal structures of gas hydrates

Pentagonal dodecahedron (a.), irregular dodecahedron (b.), tetrakaidekahedron (c.), icosahedron (d.) and hexatetrahedron (e.)

Table 2.2: Summary of some characteristics of the three crystal hydrate structures

Hydrate crystal structure	I		II		H		
Symmetry	Cubic		Cubic		Hexagonal		
Cavity	Small	Large	Small	Large	Small	Medium	Large
Cavity description	5^{12}	$5^{12}6^2$	5^{12}	$5^{12}6^4$	5^{12}	$4^35^66^3$	$5^{12}6^4$
Cell units	2	6	16	8	3	2	1
Average cavity radius[a] (Å)	3.95	4.33	3.91	4.73	3.94*	4.04*	5.79*
Variation in radius[b] (%)	3.4	14.4	5.5	1.73	4.0	8.5	15.1
Coordination number	20	24	20	28	20	20	36
nH_2O/unit cell	46		136		34		

[a]The average cavity radius varies with temperature, pressure and guest composition; [b]Variation in distance between oxygen atoms and the centre of the cage. A smaller variation in radius reflects a more symmetric cage[26]

Therefore, every mole of hydrate can retain 8 moles of CO_2. Equation 2.39 identify the total amount of hydrate formed.

$$\dot{n}_H = \frac{1}{8}\frac{dn}{dt} \tag{2.39}$$

Table 2.3: Ratio of molecular diameter to cavity diameter for few gaseous guest molecules

		$Molecular\ diameter/Cavity\ diameter$			
		Structure I		Structure II	
Guest Molecule	Diameter (Å)	5^{12}	$5^{12}6^2$	5^{12}	$5^{12}6^4$
CO_2	5.12	1.00	0.834	1.02	0.769
CH_4	4.36	0.855	0.744	0.868	0.655
N_2	4.1	0.804	0.700	0.817	0.616
O_2	4.2	0.824	0.717	0.837	0.631

Reproduced from E. Dendy Sloan, Carolyn Koh, Clathrate Hydrates of Natural Gases, Third Edition[26]

Improving the hydrate formation rate while reducing the clustering pressure, improves the CO_2 capture efficiency. This can be achieved through the use of water-miscible solvents, such as Tetrahydrofuran (THF, figure 2.6) or Tetra-n-butyl ammonium bromide (TBAB, figure 2.7), acting as a thermodynamic promoter of the hydrate formation. When the production process involves the use of these solvents, the

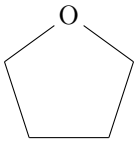

Figure 2.6: Tetrahydrofuran, THF

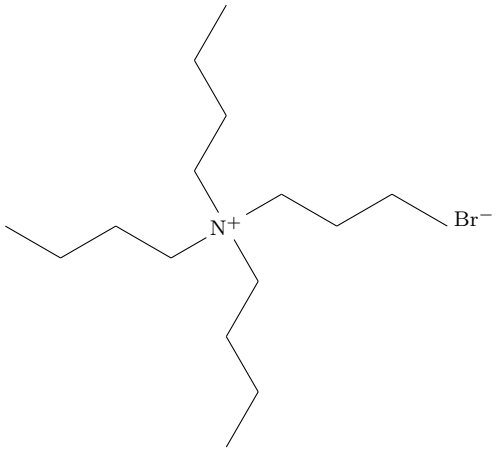

Figure 2.7: Tetra-n-butyl ammonium bromide, TBAB

formation will shift towards the type II structure, with a clathrate brute formula shown in equation 2.40. Equation 2.41 shows the less common, type III clathrate formula.

$$34\,CO_2 \cdot 136\,H_2O \tag{2.40}$$

$$6\,CO_2 \cdot 34\,H_2O \tag{2.41}$$

In general, CO_2 can form hydrates easier than other gas molecules, starting clustering at lower pressures[27]. Studies also show that, for gas mixtures of CO_2 and N_2, through the use of THF, TBAB or other promoters, the operating pressure can be lowered up to 0.2 MPa with recovery efficiencies greater than 75%[28][29][30]. The main disadvantage of this technology are the demanding operation conditions of high pressure (3 - 50 MPa) and low temperature (265 - 273 K) which lead to high energy penalties. Additives can mitigate this problem, reducing the hydrate formation pressure, speeding up the formation process. Moreover, because hydrate slurries can lead to pipe plugging, the handling of clathrates can require substantial maintenance. Assuming the treatment of a 1000 MW thermal power plant emission, in dependence of the catalyst or thermodynamic promoter used, the energy consumption for CO_2 capture through hydrates could range from 0.57 to 0.853 $kWh/kgCO_2$, accounting for a total energy penalty of 6 to 15.8%. [31][32].

2.1.5 Cryogenic Distillation

This process uses distillation at very low temperature and high pressure to separate components of gaseous mixture. In CCS, cryogenic distillation is mainly used for air separation to produce oxygen for oxyfuel combustions and to separate CO_2 from natural gas for re-injection purposes in enhanced oil recovery (EOR). This separation process depends on the difference between boiling points and volatilities of the components in the mixture. The volatility of a substance is characterised by its vapour-liquid distribution ratio shown in equation 2.42.

$$K = C_V/C_L \tag{2.42}$$

where, at a given temperature and pressure,
$C_V =$ concentration of the substance in the vapour phase
$C_L =$ concentration of the substance in the liquid phase

Greater K values are obtained for higher vapour pressures, to which correspond higher concentrations in the vapour phase. It is easier to separate mixtures with higher vapour pressure ratios; this value is also known as relative volatility (α_{ij}) and, in case of binary mixture (two component solutions), at any given temperature and pressure is given by equation 2.43.

$$\alpha_{ij} = K_i/K_j \tag{2.43}$$

The vapour pressure of a liquid increases with the temperature; the boiling point of a liquid is reached when its vapour pressure becomes equal to the surrounding pressure[6]. For CO_2 separation the process is high energy intensive, therefore it is currently discarded from the large scale implementation: the flue gas is cooled to 100 – 135 ℃; the solidified CO_2 is separated from the other light gases and it is compressed to higher pressures of 100 – 200 atm. Although being high energy demanding, recent tests show that for a typical 600 MW coal power plant, the energy needed to treat flue gas can be cut down to 88.06 MW over a total initial estimation of 195.29 MW, yielding recovery efficiencies above 90%[33].

2.1.6 Mineral Carbonation

Mineral carbonation differs from the other carbon capture methods: while the other processes previously described aim to produce a pure stream of CO_2 that needs further storage, mineral carbonation stores CO_2 in chemically stable products. Emulating the natural, slow and long-term carbon sink process of igneous rocks weathering, the obtained products have rather lower environmental impact when compared to to conventional CO_2 storage technologies (especially if compared to ocean storage). Thanks to reactions between CO_2 and oxides or silicates of magnesium, calcium and iron, this process proceeds faster than the natural one. Oxides such as CaCO and MgO are preferred since their carbonates have low solubility in water, which helps preventing ground water contamination in case of land storage. One example of these reactions is given in equation 2.44.

$$MgO + CO_2 \longrightarrow MgCO_3 + \text{heat} \tag{2.44}$$

In carbonates, carbon atoms are in their lowest energy state and it gives these products stability over geological time scales (the retention time can be greater than 100000 years). Carbonation reactions are exothermic, proceed at room pressure and temperature releasing the excess energy as heat and, although thermodynamically favoured, they have slow reaction rates. Another major issue is the need of 2 - 3 ton of oxides (rare in nature due to their reactivity) per tonne of captured CO_2. Unless a fix to these issues is found, for example chemically optimise the process, this solution is not viable for industrial applications[6].

2.2 Clathrate-based separation

This section focuses on the clathrate-based separation for CO_2 capture. As mentioned in section 2.1.4, hydrate-based separation is a relatively new technology for CO_2 capture: a flue gas mixture passes through chilled water at at high pressure and low temperature; CO_2 molecules freeze with the water molecules and get trapped into solid crystalline cage-like structures known as clathrates. CO_2 and H_2O freeze together forming a slurry of ice crystals in liquid water together with other gas components non trapped in the ice crystals. The hydrates containing CO_2 molecules are separated from the other components for storage or transport purposes. CO_2 is recovered by heating the slurry, therefore breaking the ice cages and releasing the gas molecules[22].

2.2.1 Process Description

Clathrate formation happens in supersaturation conditions and can be divided into three steps:

- Nucleation
- The solute is transferred to the hydrate surface
- The solute is incorporated into the hydrate matrix

Consider the situation shown in figure 2.8. At a temperature T_1 and concentration a the solution is under-saturated and all the hydrate crystals dissolve. In b, the saturated solution is in equilibrium with the crystals. In c the solution is in the metastable region where crystals can grow but cannot nucleate, therefore in absence of crystals there will not be any crystal formation. Spontaneous crystals nucleation occurs on the metastable limit, in point d (small crystals invisible to the naked eye). The supersaturation condition is the concentration difference between points c and b, $\Delta c = c - c_s$, while its supersaturation limit is $\Delta c_{limit} = c_m - c_s$. The difference between the temperatures at points e and c is the supersaturation temperature difference (about 2 °F). The limit of the supersaturation temperature difference is difference between temperatures at points f and d. If a fluid is cooled down slowly without agitation it is possible to supersaturate the solution[34]. The nucleation can be homogeneous or heterogeneous: ho-

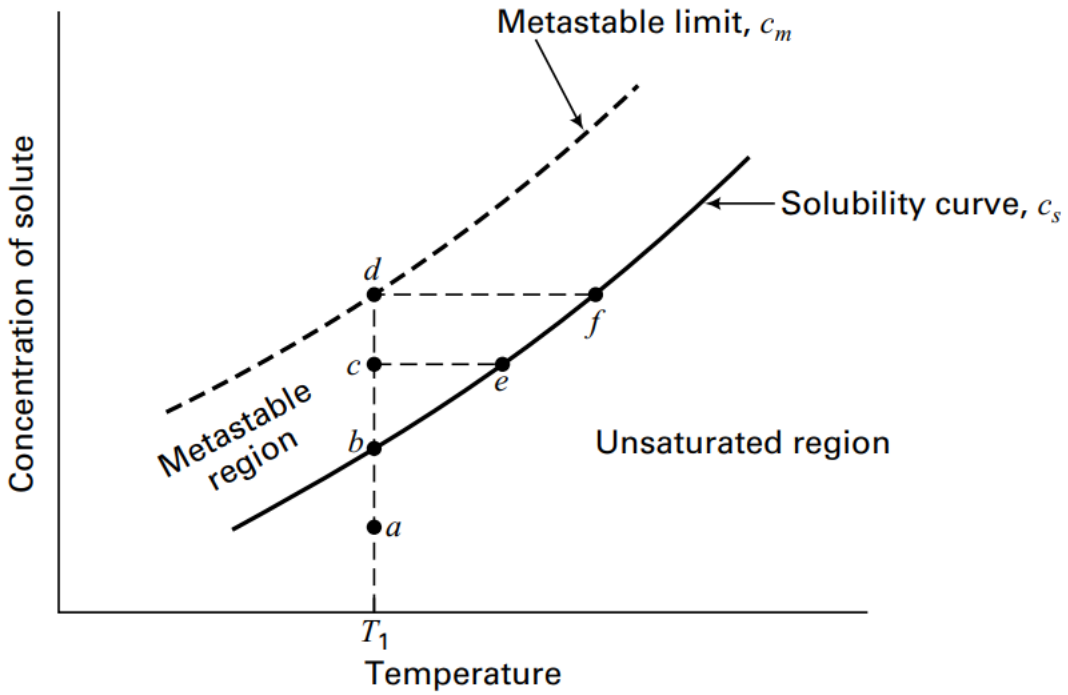

Figure 2.8: Representative solubility–supersolubility diagramn
Reproduced from E. Dendy Sloan, Carolyn Koh, Clathrate Hydrates of Natural Gases, Third Edition [34]

mogeneous nucleation occurs when there is no presence of other particles in the solution; we talk about heterogeneous nucleation when in the presence of other particle in the solution. Another differentiation can be made between primary and secondary nucleation. Primary nucleation occurs in the absence of previously formed hydrates while secondary nucleation is the origination of new nucleates after other hydrate structures are already present. The Gibbs free energy plays an important role in the crystals nucleation: under supersaturated conditions the dissolved gas free energy is higher than the one of the hydrate. This condition favours the new hydrates nucleation but requires the formation of an interface. The Gibbs free energy of the interface (ΔG_s) is higher than the one in the bulk (ΔG_v) and both values depend on the cluster size[35]. The two terms have opposite signs. ΔG_s dominate in the beginning preventing crystals nucleation, growing with the square of the cluster radius, while ΔG_v grows with the cluster volume (see figure 2.9). Equation 2.45 shows the Gibbs free energy equation of the system.

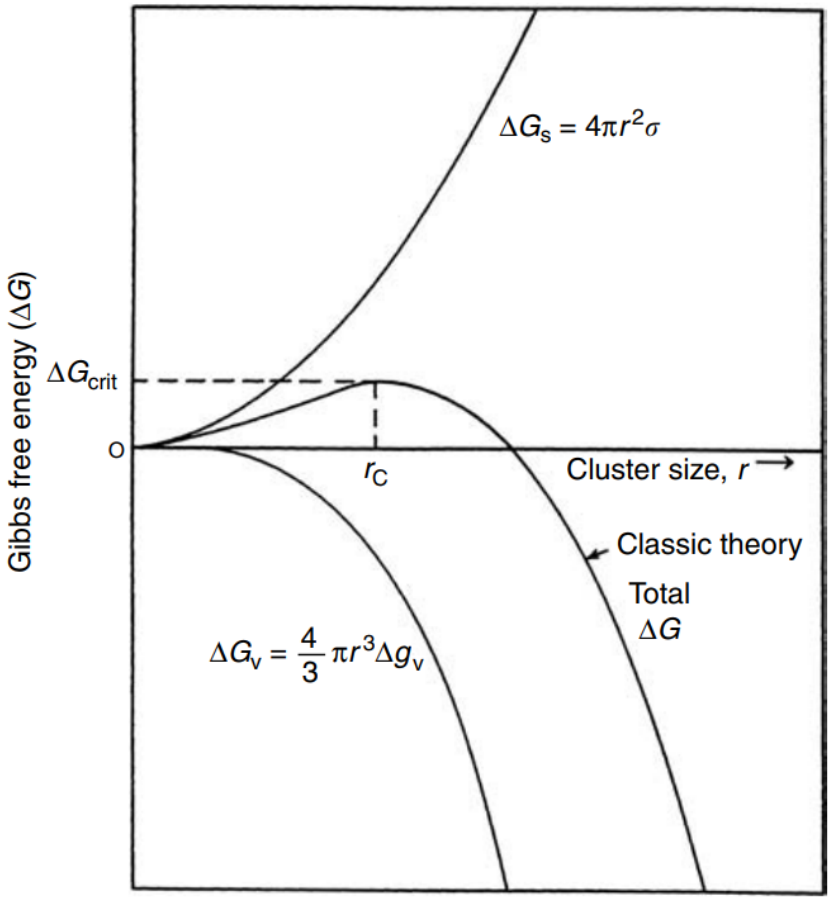

Figure 2.9: Surface free energy (ΔG_s) and bulk free energy (ΔG_v) as functions of cluster size
Reproduced from E. Dendy Sloan, Carolyn Koh, Clathrate Hydrates of Natural Gases, Third Edition [34]

$$\Delta G = \Delta G_s + \Delta G_v = 4\pi r^2\sigma + \frac{4}{3}\pi r^3 \Delta g_v \tag{2.45}$$

Where

$\Delta g_v =$ Free energy change per unit volume

$\sigma =$ Surface tension at the hydrate-liquid interface

With the assumption of full occupancy and ideal solution, Δg_v is):

$$\Delta g_v = \frac{RT_{exp}}{V_{mol,H}}[ln(\frac{x^{int}}{x^{tb}}) + \eta ln(\frac{1-x^{int}}{1-x_{tb}})] \tag{2.46}$$

Where

$R =$ Universal gas constant

$T_{exp} =$ Experimental temperature

$V_{mol,H} =$ Hydrate molar volume

$\eta =$ Hydrate occupancy

$x^{int} =$ CO_2 equilibrium concentration

$x^{tb} =$ CO_2 concentration at turbidity

The Gibbs free energy reaches the maximum when the critical growth radius is reached (equation 2.47).

$$r_c = \frac{-2\sigma}{\Delta g_v} \tag{2.47}$$

Therefore, for the critical Gibbs free energy we have:

$$\Delta G_{crit} = \frac{4}{3}\pi\sigma r_c^2 \tag{2.48}$$

The nucleation time (equation 2.49) is defined as the time interval between the moment the supersaturated condition is established and the moment the first clusters with $r = r_c$ is formed. The nucleation time depends on various parameters such as operating temperature and stirring rate. A positive variation on the operating temperature can significantly increase the nucleation time, while an increase in the stirring rate decrease the nucleation time[35]. The driving force for CO_2 hydrate nucleation is defined as the difference between the fugacity of the molecule in the liquid phase at experimental conditions (f_{CO_2}) and the three phase equilibrium fugacity of the molecule in the hydrate phase at experimental temperature and pressure(f_H)[36].

$$t_{nuc} = K[\frac{f_{CO_2}(T,P)}{f_H(T,P)} - 1]^{-j} \tag{2.49}$$

where K and j are parameters varying with the nature of the guest molecule and on the type of reactor. The reaction rate of hydrate formation has been reported to be mainly influenced by the operating temperature: the reaction rate constant has an Arrhenius-type relationship with the temperature, increasing with it[37]. The main product of the reaction is a slurry of clathrates, water and other non caged gas molecule. Without the use of catalysts or thermodynamic promoters, as mentioned in section 2.1.4, the formation of type I structure dominates (2.38), while using catalysts and promoters, the formation will shift towards the type II structure (2.40). Structure of the type III (2.41) are less common. Considering the full occupancy of the clathrate cages, every mole of hydrate can retain 6, 8, or 34 moles of CO_2 in dependence of the formed structure type. Equation 2.50 identify the total amount of hydrate formed.

$$\dot{n}_H = \frac{1}{S}\frac{dn}{dt} \tag{2.50}$$

S can vary up to a maximum of 34 in case of structures type II. The clathrates are separated from the water portion for transport and storage, but part of them could remain in the system. Equation 2.51 shows the total amount of hydrate present:

$$\dot{n}_{tot} = \dot{n}_H + \dot{n}_{sys} \tag{2.51}$$

Where $\dot{n}_{sys}$ is the amount of hydrates which remains in the system. The hydrates total weight per second can be calculated as:

$$\dot{m}_H = \dot{n}_{tot} MW_H \tag{2.52}$$

Where MW_H is the hydrate molecular weight. The hydrate mass fraction in the slurry is calculated as:

$$x_H = \frac{\dot{m}_H}{\dot{m}_{tot}} \tag{2.53}$$

The slurry density ρ_s can also be used to determine the amount of hydrates formed:

$$\rho_s = \frac{\rho_{sol}\rho_H}{\rho_{sol}w_H + \rho_H(1 - w_H)} \tag{2.54}$$

where

$w_H =$ Hydrate mass fraction in the slurry

$\rho_H =$ Hydrate density

$\rho_{sol} =$ Density of the solution

It is important to note that the hydrate formation is an exothermic process and this works against the crystal growth, therefore the generated heat must be removed. In order to produce a pure stream of CO_2, one viable option is the utilisation of the heat of reaction in a cross heat exchanger to break the Van Der Waals interaction forces between the molecules and the hydrogen bonds, releasing the gas molecules. The hydrate heat of dissociation is given by the Clausius-Clapeyron equation (2.55)[37]:

$$\frac{dlnP^{int}}{d(\frac{1}{T})} = \frac{-\Delta H_d}{zR} \tag{2.55}$$

Where

$P =$ Absolute hydrate pressures at equilibrium with vapour and liquid water

$T =$ Absolute hydrate temperature at equilibrium with vapour and liquid water

$R =$ Universal gas constant

$z =$ Gas compressibility

Most of the research on CO_2 hydrates focuses on semi-bath processes and, although there are studies in literature on continuous hydrate production, the experimental data retrieved from scientific papers consulted presents numerous incongruities[2]. Nevertheless, the feasibility analysis of a clathrate capture system was carried on and is described in detail in chapter 3.

2.3 Summary of key findings

Due mainly to the commercial deployment and development of the technology in the industrial sector and due to the chance of virtually retrofit any existing power plant, the choice of this analysis falls on the post-combustion treatment of flue gases. Here is a summary of important aspects on the technologies analysed.

- When aiming at CO_2 removal at low partial pressure, amine absorption systems can reach removal

[2]On top of that, none of the scientists contacted answered questions related to their research.

rates higher than 90%[8][9][10]. This is the most diffused CO_2 capture technology on an industrial scale with a high selectivity, making it very suitable for CO_2 separation.

- Physical adsorption through Pressure Swing Adsorpion (PSA) or Temperature Swing Adsorption (TSA) is aso a viable option: PSA for CO_2 recovery is already a commercially available technology that yields efficiencies above 90%[15][16]; TSA is also a promising technology that, although has a longer regeneration time, yields CO_2 purity higher than 95%, with recovery higher than 80%[17].
- Due to the constant advancement in membrane separation technologies, it is currently possible to yield separation efficiencies above 90% with product purity up to 95%[18][19]. Unfortunately, this technology is heavily affected by the flue gas low pressure and CO_2 concentration ($\sim$15%) which translate into a low CO_2 permeation driving force.
- Cryogenic distillation can yield recovery efficiencies above 90%, but it is high energy intensive, therefore it is currently discarded from the large scale implementation[33].
- Mineral carbonation reactions have slow reaction rates and need 2 - 3 tonnes of oxides (rare in nature due to their reactivity) per tonne of captured CO_2. Unless a solution to these issues is obtained, this solution is not viable for industrial applications[6].
- Hydrate separation technology has great potential for future implementations. Assuming the treatment of a 1000 MW thermal power plant emission, the energy consumption for CO_2 capture through hydrates could range from 0.57 to 0.853 kWh/kg-CO_2, accounting for a total energy penalty of 6 to 15.8%[31][32]. The main disadvantage of this technology are the demanding operation conditions of high pressure (3-50 MPa) and low temperature (265-273K) which lead to high energy penalties. Additives can mitigate this problem, reducing the hydrate formation pressure up to 0.3 MPa, speeding up the hydrate formation process. Moreover, because hydrate slurries can lead to pipe plugging, the handling of clathrates can require substantial maintenance.

With this in mind, the analysis on a process implementing hydrate capture technology and its comparison with the amine absorption proceeds in the following chapters.

Chapter 3

Process Model

This chapter describes the tool used to simulate the hydrate-based CO_2 capture process explained in chapter 2. It describes the adopted methodology and the plant layout.

3.1 Process Simulation Tool: ASPEN-Plus

The process was modelled and simulated through Aspen Plus V8.4®. ASPEN-Plus is a process modelling tool that allows the user to design, optimise, and monitor the performance of a wide variety of chemical and process engineering processes. It is possible to create ad-hoc models by designing the plant flow-sheet and specifying operation conditions and chemical components. The software analyses all the specifications and executes the necessary calculations listing the results per component and per each stream[3]. The choice of this software was made because of several relevant reasons:

- it provides the world's largest database on pure component and phase equilibrium for conventional chemicals, polymers, electrolytes and solids;
- it receives regular data updates from the NIST (National Institute of Standards and Technology);
- it has a comprehensive library of unit operation models addressing a variety of processing equipment (solid, liquid, and gas);
- the Aspen Custom Modeller (APC) allows the user to build user-defined models and libraries.

3.2 Methodology

The work consisted first on the analysis of the current state-of-the-art technologies for CO_2 capture (chapter 2). Afterwards, the most advanced and commercially developed was identified (section 2.3) for

[3]Although being a great tool for process engineering with several equation models and extensive database, ASPEN-Plus is not optimised for reactions involving solid-liquid and solid-gas equilibrium phases. Because of this, during the simulation runs, several issues were encountered which will be mentioned in the next sections.

a comparison with the hydrate-based separation. The clathrate process was then modelled[4] in order to be comparable with the MEA-based plant showed in chapter 4. The designed process reliability was assessed by using operation conditions, estimations and hypothesis reported in the scientific literature analysed. Afterwards, the energy comparison between the amine process and the hydrate-based one was discussed together with an initial cost analysis for the clathrate system. Finally, conclusions were drawn.

3.2.1 ELECNRTL model

In order to correctly model the plant scheme, the right set of equations must be chosen. ASPEN-Plus has several equation models to choose from and, in dependence of the operating conditions, components and reactions, some of them result to be a better choice than others. In the hydrate formation, a method that can describe correctly the solubility of CO_2 in water and the respective interaction between each molecule is of crucial importance, therefore the process was analysed on the basis of a non-random two-liquid model (NRTL). This is an activity coefficient model correlating, for each component, activity coefficients and its molar fraction in the concerned liquid phase. The NRTL model equation is:

$$\ln y_{\text{i}} = \frac{\sum_j x_j \tau_{ji} G_{ji}}{\sum_k x_k G_{ki}} + \sum_j \frac{x_j G_{ji}}{\sum_k x_k G_{ki}} (\tau_{ij} - \frac{\sum_m x_m \tau_{mj} G_{mj}}{\sum_k x_k G_{kj}}) \tag{3.1}$$

where

$G_{ij} = e^{-\alpha_{ij}\tau_{ij}}$

$\tau_{ij} = a_{ij} + {}^{b_{ij}}/_{T} + e_{ij} \ln T + f_{ij} T$

$\alpha_{ij} = c_{ij} + d_{ij}(T - 273.15K)$

$\tau_{jj} = 0$

$G_{jj} = 1$

$T =$ Temperature

$x_j =$ Mole fraction of the component j

$x_k =$ Mole fraction of the component k

The parameters a_{ij}, b_{ij}, c_{ij}, d_{ij}, e_{ij} and f_{ij} are determined from VLE (Vapour-Liquid Equilibrium) and/or LLE (Liquid-Liquid Equilibrium) data regression using the Dortmund Databank. It is important to note that a_{ij}, b_{ij}, e_{ij} and f_{ij} are unsymmetrical, therefore a_{ij} may not be equal to a_{ji}. The method uses user input units for temperature, however, if any of a_{ij}, b_{ij}, d_{ij} or e_{ij} is different from *0*, absolute temperature units are assumed for b_{ij}, d_{ij}, e_{ij} and f_{ij}. In particular, 3 values are used for c_{ij}: *0.30* for non-polar substances, non-polar substances with polar non-associated liquids and in case of small deviations from ideality; *0.20* for saturated hydrocarbons with polar non-associated liquids and systems that exhibit liquid-liquid immiscibility; *0.47* for strongly self-associated substances with nonpolar substances.

[4]This work was primarily based on a pilot plant research going on in Porto, a city in the north of Portugal. Therefore, the initial idea was to use that pilot plant scheme in order to assess the feasibility of that particular studied set-up. Although data was readily available, because of some unexpected issue no information was released on the process and everything was based on a theoretical approach with conservative assumptions.

τ_{ij}, τ_{ji} and τ_{mj} are dimensionless parameters related to the interaction energy parameters G_{ij}, G_{ji} and G_{mj}[38]. The ELECNRTL property method was chosen because considered the most versatile property method for this analysis. It can handle very low and very high concentrations whether dealing with aqueous or mixed solvent systems. The ELECNRTL is fully consistent with the NRTL-RK property method: a non-random two-liquid model that incorporate the Redlich-Kwong equation of state. The molecular interactions for this method are calculated exactly like the ones of the NRTL-RK, therefore the ELECNRTL can use the same databank for binary molecular interaction parameters. Many binary and pair parameters and chemical equilibrium constants from regression of experimental data are included in Aspen Physical Property (APP) system databanks. The solubility of supercritical gases can be modelled using Henry's law. Heats of mixing are calculated using the electrolyte NRTL model. The Redlich-Kwong equation of state is used for all the vapour phase thermodynamic properties in the NRTL-RK method[39]. The equation for the method is:

$$P = \frac{RT}{V_m - b} - \frac{a/T^{0.5}}{V_m(V_m + b)} \tag{3.2}$$

where

$\sqrt{a} = \sum_i x_i \sqrt{a_i}$

$b = \sum_i x_i b_i$

$a_i = {0.42748023 R^2 {T_{ci}}^{2.5}}/{p_{ci}}$

$b_i = {0.42748023 R T_{ci}}/{p_{ci}}$

$P =$ Pressure

$x_i =$ Mole fraction of the component i

$T =$ Temperature

$R =$ Universal gas constant

$V_m =$ Molar Volume

a and b are constant used for molecule attractive potential and volume corrections. The molar Gibbs free energy (G_m^*) is calculated as:

$$G_m^* = x_w \mu_w^* + \sum_s x_s \mu_s^{*,l} + \sum_k x_k \mu_k^\infty + RT \sum_j x_j ln_j + G_m^{*,E} \tag{3.3}$$

Where the subscripts m, w, s, k, and j refer, respectively, to molar, water, non-water solvent, ion/molecule solute and any component. Both, molar Gibbs free energy G_m^* and molar excess Gibbs free energy $G_m^{*,E}$ are calculated according the asymmetrical reference state (marked with $*$): pure water and molecular solutes and ions at infinite dilution. The water thermodynamic potential μ_w^* (Gibbs free energy for pure water, also marked with *) is a function of the ideal gas departure function and heat capacity and is calculated accordingly. The departure function is defined as the difference between the ideal potential and the real potential at a specified pressure and temperature ad it is obtained from the ASME steam tables.

$$\mu_w^* = \mu_w^{*,ig} + (\mu_w^* - \mu_w^{*,ig}) \tag{3.4}$$

μ_k^∞ is the aqueous infinite dilution potential and it is calculated from the heat capacity polynomial model for infinite dilution aqueous phase. In case the necessary parameters are missing, the Criss-Cobble model for ionic solutes is used (equation 3.5, 3.6 and 3.7):

$$\mu_k^\infty = H_k^\infty - TS_k^\infty + RTln(\frac{1000}{M_w}) \tag{3.5}$$

$$H_k^\infty = \Delta_f H_k^{\infty,aq} + \int_{298.15}^{T} C_{p,k}^{\infty,aq} dt \tag{3.6}$$

$$S_k^\infty = \frac{\Delta_f H_k^{\infty,aq} - \Delta_f G_k^{\infty,aq}}{298.15} + \int_{298.15}^{T} \frac{C_{p,k}^{\infty,aq}}{T} dt \tag{3.7}$$

The terms H_k^∞ and TS_k^∞ are molality based, therefore $RTln(\frac{1000}{M_w}$ is added for the conversion. In case the parameters necessary to calculate $C_{p,k}^{\infty,aq}$ (the aqueous infinite dilution heat capacity) are missing, Henry's law is used:

$$\mu_k^\infty = \mu_k^{*,ig} + RTln(\frac{H_{k,w}}{p^{ref}}) \tag{3.8}$$

where

$H_{k,w} =$ Solubility constant

$p^{ref} =$ Reference pressure

The non-water solvent contribution $\mu_s^{*,l}$, the ideal mixing term ($RT\sum_j x_j ln_j$)and molar excess Gibbs free energy $G_m^{*,E}$ are calculated according the equation model NRTL activity coefficient model.

3.2.2 ASPEN-Plus Simulation of Clathrate Formation

It is important to notice that with the use of a thermodynamic promoter, such as THF, the formation of structure of type II dominates the product of the reaction. Considering full occupancy of the hydrate cavities, the ratio between CO_2 and H_2O molecule is $1/4$[5]. In the simulations, only structures type I and II were defined, *8 CO_2 · 46 H_2O* and *34 CO_2 · 136 H_2O* respectively. Although, due to several issues encountered while running simulations with the structure type II, a first approximation was deemed necessary: the formation of solely structure type I with full occupancy of its cavities was considered in the reaction products. The full occupancy of the cavities was assumed to partially compensate the difference in needed water between the 2 clathrate structure in terms of CO_2 captured; this might lead to an overestimation of the equipment size and, consequently, of the net power needed. The simulation tool had no inbuilt template on clathrates, therefore all the required data to define the clathrate were manually implemented in order to ensure reliable result in the energy calculations.

3.2.3 Data used

This section summarise the main parameters used to run the simulation. The data is based on a 900 MW super-critical power plant unit that vents to the atmosphere 824.2 kg/s of flue gas[41]. Table 3.1

[5]Despite using catalysts or thermodynamic promoters, many of the consulted documents consider the formation of structure type I with a molar ratio of $1/5.75$. Some other consider the formation of hydrate with different molar ratio, such as $1/7.3$[40].

shows the gas composition. According to laboratory tests, using of a tetrahydrofuran (THF) solution 5%

Table 3.1: Flue gas composition

Component	N_2	CO_2	SO_2	O_2	H_2O	Ar
Mole fraction	0.7378	0.1416	0.0009	0.0329	0.0780	0.088

molar for the reaction of a pure CO_2 stream at the operating conditions of 10 ℃ and 8 bar releases 108.7 kJ/mol of clathrate formed[42]. The equilibrium of solutions at various THF concentrations, with gas compositions close to the one of the flue gas stream in exam (16.9% CO_2 and 83.1% N_2), were also studied[43]. Figure 3.1 shows the incipient hydrate formation conditions for different THF concentration, for which infinitesimal amount of hydrate crystals are in equilibrium with gas and aqueous phases. The

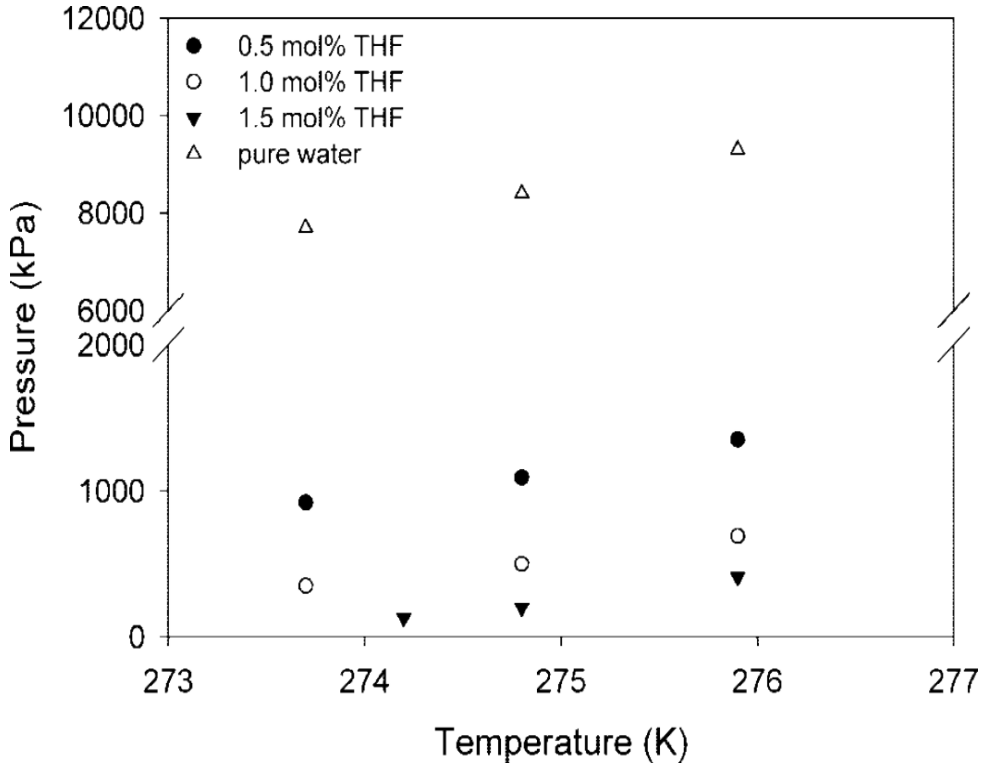

Figure 3.1: Incipient hydrate formation equilibrium. 16.9% CO_2, 83.1% N_2
Reproduced from Praveen Linga, Adebola Adeyemo and Peter Englezos, Medium-Pressure Clathrate Hydrate/Membrane Hybrid Process for Postcombustion Capture of Carbon Dioxide[43]

tests revealed that the use of THF 1% molar allows for the hydrate reaction to proceed at pressure as low as 10 bar, but it is possible to increase the total number of moles consumed by increasing the operating pressure. They state that, with their initial gas composition, 23 bar is the optimal pressure to obtain an hydrate product with a CO_2 fraction of 98%[6][43]. A conservative approach is adopted for the simulation runs: taking into account the different gas composition a solution 5% mol of THF is used, setting a temperature of -1 ℃ and a pressure of 30 bar for the reactor. Even thought it is theoretically possible for the reaction to proceed at higher temperature and pressure, the vessel needs to host already hydrate crystals which function as nucleation initiators. If this condition is not respected, the thermodynamic

[6]This was possible using a series of 3 hydrate formation stages.

conditions are not enough for the clustering reaction to proceed. Table 3.2 lists the design general parameters while 3.3 shows the reactor parameters. The CO_2 capture efficiency of the overall process was set to 90%[44]. As mentioned before, nitrogen needs noticeably higher pressures to form hydrates

Table 3.2: Design general parameters

Stream	Mass flow [kg/s]	Temperature [℃]	Pressure [bar]
Flue gas	824.2	45	1
THF	148	15	1
Water	332	15	1

Table 3.3: Reaction parameters with THF 5% molar

Enthalpy of reaction (10 ℃, 5 bar) [kJ/mol]	108.7
Temperature [℃]	-1
Pressure [bar]	30

therefore N_2 clathrates were not included in the product stream[7]. The other components in the flue gas are assumed non-influential on the clathrate production. The next section (3.2.4) describes briefly the simplified flow scheme of the designed plant, detailed later in section 3.2.5.

3.2.4 Plant Layout

The simplified plant layout is shown (figure 3.2). The complete scheme has a similar layout, with the flue gas mass-flow divided into 5 streams and treated in 5 equal, parallel systems. Although this set-up increases the plant capital cost, the subdivision is needed to operate with smaller mass flows, which might lower the operation and maintainment costs and help in future works related to sizing and optimisation of the plant equipments. The full scheme can be consulted in appendix A. In order for the reaction to take place, the feed streams must be brought to the required operating condition (30 bar and -1 ℃). Before entering the reactor, the flue gas (FLUE) passes trough a series of 3 inter-cooled compressions (COMPR1,2 & 3 + HEATEX1,2 & 5) while water (H2O-IN) and tetrahydrofuran (THF) are brought to the required pressure thanks to a pump (PUMP1). Both flows mix and pass through additional cooling units (HEATEX3 & 4) to reach the required temperature. The cooled and pressurised feeds enter the reactor (REACTOR) in which the clathrate crystallisation reaction takes place. Part of the water exiting the heat exchanger (HEATEX3) is used to keep the reactor at a constant operating temperature. This coolant water is then pressurised and expands in turbine (TURB-VAP) generating power supplied to the necessary utilities. The reactor output is a slurry containing a mixture of clathrates, water, thermodynamic promoter and non reacted gases. The slurry gets then separated (SPLIT-H) in a gaseous, liquid and mixed fraction using part of the residual heat from the reactor. The separated gas (GAS-OUT) expands

[7] The pressure needed to form N_2 hydrates can be higher than 160 bar[27].

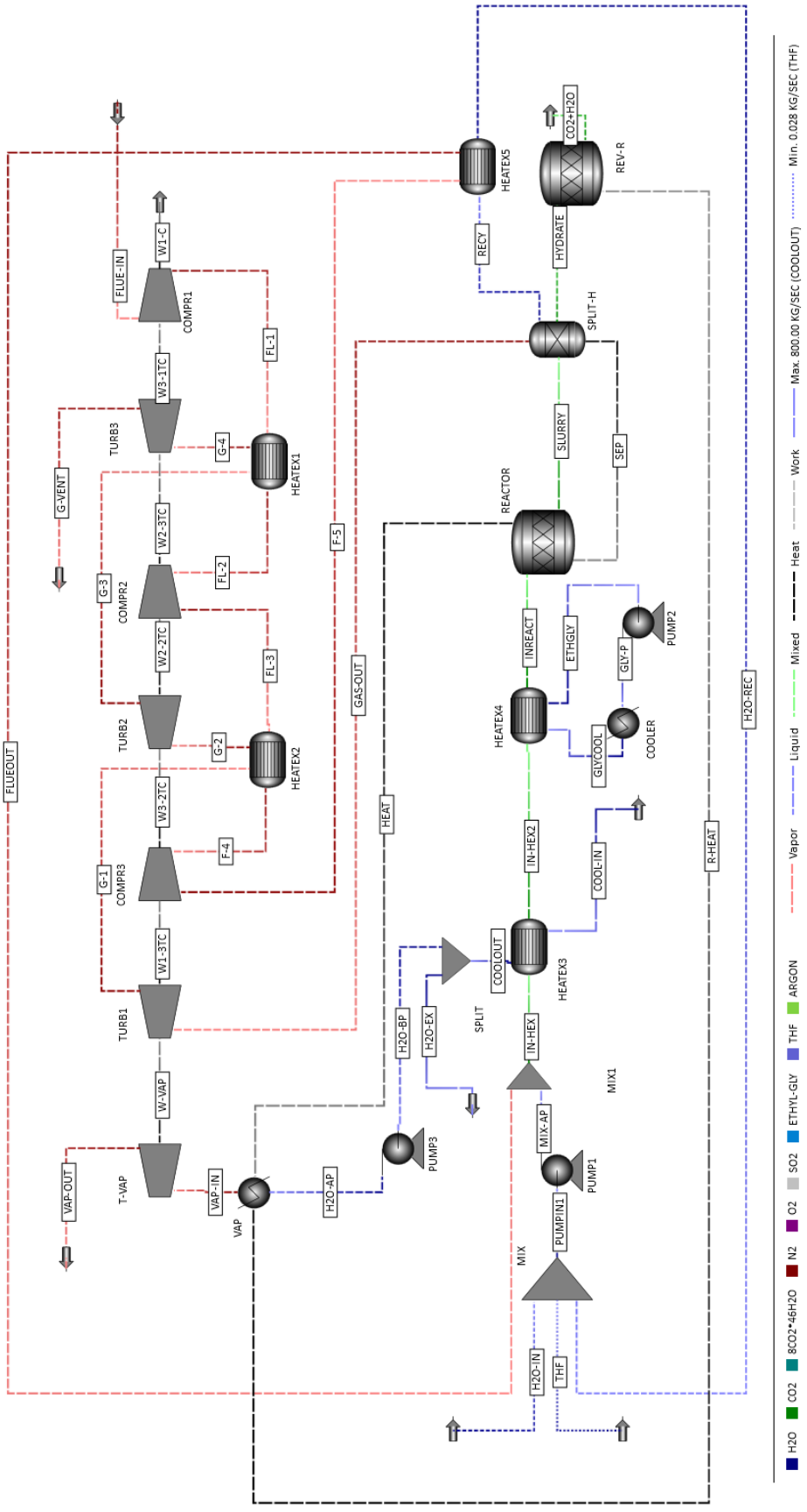

Figure 3.2: Process flow scheme for hydrate-based CO_2 capture from flue gas

in a series of 3 inter-heated turbine cycles (TURB1,2 & 3 + HEATEX1 & 2) before being vented to the atmosphere, supplying, partially, the power needed by the compressors. The liquid fraction (H2O-REC) is recirculated to the water feed stream. The mixed stream (HYDRATE) is heated with the residual heat of the reaction to obtain a pure stream of CO_2 and water[8].

3.2.5 Equipment Analysis

This section describes the plant equipment shown in figure 3.2. The separation system consists of the following equipment:

COMPR1,2 & 3 The flue gas needs to be compressed to 30 bar before entering the reactor and participating to the reaction. The pressure is reached with three inter-refrigerated isentropic compressions. The compression ratio is set to 3.11, chosen in accordance with the conventional rules of thumbs that prevent compressor damage and related issues caused by the excessive raise in temperature or liquid droplets formation[45]. The compression efficiency is set to 80%.

TURB1,2 & 3 The non-captured gaseous fraction (mainly N_2) is expanded in 3 inter-heated expansions before being vented to the atmosphere. As for the compressions, the pressure ratio was chosen according conventional rules and set to 0.3[45]. Part of the power needed by the compression cycle is obtained through the turbine expansions, which efficiency is set to 80%.

HEATEX1,2 & 5 Three heat exchangers cool the compressed flue gas and heat the exhaust gas fraction (mainly N_2) in contemporary. All the heat exchangers are considered as shell and tubes, operating in counter-current flow with a specific temperature approach of 5 ℃ to avoid temperature crossing. The heat transfer coefficient is set to 0.028 kW/m^2K for both HEATEX1 & 2 (gas-gas) while for HEATEX5 (gas-mixed phase) the value 0.17 kW/m^2K was chosen[45]. Pressure losses are set to 0.

PUMP1,2 & 3 The liquid fraction entering the cycle is pressurised to 30 bar with a first centrifugal pump (PUMP1). The second pump (PUMP2) is used in the refrigerating cycle to pressurise the ethylene-glycol solution to 2.5 bar[44]. PUMP3 pressurises to 50 bar the water fraction sent to the vaporiser (VAP) for the expansion in turbine (TURB-VAP). Whether for the inlet fraction, the vaporisation or the refrigeration, the pumping efficiency is set to 80%.

TURB-VAP The vaporised water fraction (450 ℃ and 50 bar) expands in turbine generating the greatest amount of power supplied to the needed utilities. The vapour exiting the turbine (216 ℃ and 6 bar) could be used for co-generation purposes or as another heating source. The pressure ratio was chosen according conventional rules and set to 0.12[45].

[8] Another option is to directly send the hydrate fraction to the storage facility.

HEATEX3 & 4 The reactor feed stream is cooled with 2 shell and tubes heat exchangers operating in counter-current flow. HEATEX2 uses water as coolant fluid with a specific temperature approach set to 5 °C. HEATEX3 is cycled with a solution 30%mol of ethylene-glycol with a hot side outlet temperature set to -1 °C. The heat transfer coefficient is set to 0.57 kW/m^2K for both HEATEX3 (water-mixed phase) and to 0.74 kW/m^2K for HEATEX4 (brine-mixed phase)[45]. Pressure losses are set to 0.

COOLER After cooling the mixed feed of flue gas, water and THF, the ethylene-glycol is brought back to the required temperature (21 °C) by a refrigeration process thanks to a cooling unit.

REACTOR The reactors operate at 30 bar and -1 °C. the temperature is kept constant using part of the cooling water recirculated from the heat exchanger (HEATEX3). The CO_2 conversion rate is set to 0.9 and the energy released by the hydrate formation in presence of the 5%mol THF solution is calculated by the simulator engine. The calculations are based on the same THF concentration and a pure stream of CO_2 at 10 °C and 5 bar (-108.7 kJ/mol)[42]. The other gases are considered to non influence the reaction products.

SPLIT-H The slurry coming out of the reactor is separated into 3 streams, gaseous (GAS-OUT), liquid (RECY) and mixed phase(HYDRATE). The gaseous stream is composed by nitrogen (93%), the CO_2 not captured and the other non-reagent gases; the liquid fraction is composed by water and THF and is recirculated to the initial feed stream (IN-HEX); the mixed stream is composed by the hydrate solid fraction and a liquid fraction of water and THF (0.1%). Part of the energy released by the hydrate formation is used for the separation process.

REV-R This piece of equipment is optional and is here because it is the only way to simulate the clathrate dissociation reaction. Heat is required for the reverse reaction to take place: part of the heat obtained from the main reaction is harvested for this purpose.

MIX & MIX1 These pieces of the plant serve solely the purpose of identify the recirculated stream mixing before the entrance of PUMP1 and HEATEX3.
Table 3.3 summarises the flows main parameters and their related equipment for each parallel system.

Table 3.4: Equipment flows main parameters

Block	Direction	Stream	Mass flow [kg/s]	Temperature [°C]	Pressure [bar]
COMPR1	IN	FLUE	164.8	45	1
	OUT	FL-1	164.8	185.3	3.11
COMPR2	IN	FL-2	164.8	132.7	3.11
	OUT	FL-3	164.8	306.5	9.7

Table 3.4 – *Equipment flows main parameters (continues on the next page)*

Table 3.4 – *Equipment flows main parameters (continued from the previous page)*

COMPR3	IN	FL-4	164.8	154.9	9.7
	OUT	FL-5	164.8	337.1	30.1
COMPR3	IN	FL-4	164.8	154.9	9.7
	OUT	FL-5	164.8	337.1	30.1
TURB1	IN	GAS-OUT	125.6	0.05	30
	OUT	G-1	125.6	-63.6	9.45
TURB2	IN	G-2	125.6	144.9	9.45
	OUT	G-3	125.6	51.2	3
TURB3	IN	G-4	125.6	122.7	3
	OUT	G-VENT	125.6	34	0.9
HEATEX1	IN-HOT	FL-1	164.8	185.3	3.11
	OUT-HOT	FL-2	164.8	132.7	3.11
	IN-COLD	G-3	125.6	51.2	3
	OUT-COLD	G-4	125.6	122.7	3
HEATEX2	IN-HOT	FL-3	164.8	306.5	9.7
	OUT-HOT	FL-4	164.8	154.9	9.7
	IN-COLD	G-1	125.6	-63.6	9.45
	OUT-COLD	G-2	125.6	144.9	9.45
HEATEX3	IN-HOT	IN-HEX	364.8	93.5	30.1
	OUT-HOT	IN-HEX2	364.8	45.5	30.1
	IN-COLD	COOL-IN	900	15	1
	OUT-COLD	COOLOUT	900	35.5	1
HEATEX4	IN-HOT	IN-HEX2	364.8	45.5	30.1
	OUT-HOT	INREACT	364.8	-1	30.1
	IN-COLD	GLYCOOL	370	-21	2.5
	OUT-COLD	ETHGLY	370	44.1	2.5
MIX	IN	H2O-IN	65.43	15	1
		THF	0.07	15	1
		H2O-REC	134.5	103.2	30
	OUT	PUMPIN1	200	68	1
PUMP1	IN	PUMPIN1	200	68	1
	OUT	MIX-AP	200	68.7	32
MIX1	IN	MIX-AP	200	68.7	32
		FLUEOUT	164.8	113.2	30.1
	OUT	IN-HEX	364.8	93.5	30.1

Table 3.4 – *Equipment flows main parameters (continues on the next page)*

Table 3.4 – *Equipment flows main parameters (continued from the previous page)*

SPLIT	IN	COOLOUT	900	35.5	1
	OUT	H2O-EX	757.8	35.5	1
		H2O-BP	142.2	35.5	1
PUMP3	IN	H2O-BP	142.2	35.5	1
	OUT	H2O-AP	142.2	36	50
VAP	IN	H2O-AP	142.2	36	50
	OUT	VAP-IN	142.2	450	50
TURB-VAP	IN	VAP-IN	142.2	450	50
	OUT	VAP-OUT	142.2	216.8	6
REACTOR	IN	INREACT	364.8	-1	30.1
	OUT	SLURRY	364.8	-1	30
SPLIT-H	IN	SLURRY	364.8	-1	30
	OUT	HYDRATE	104.7	0.05	30
		RECY	134.5	0.05	30
		GAS-OUT	125.6	0.05	30
HEATEX5	IN-HOT	FL-3	164.8	306.5	9.7
	OUT-HOT	FLUEOUT	164.8	113.2	30.1
	IN-COLD	RECY	134.5	0.05	30
	OUT-COLD	H2O-REC	134.5	103.2	30
REV-R	IN	HYDRATE	104.7	0.05	30
	OUT	CO2+H2O	104.7	94.8	1
PUMP2	IN	ETHGLY	370	44.1	2.5
	OUT	GLY-P	370	44.1	2.5
COOLER	IN	GLY-P	370	44.1	2.5
	OUT	GLY-COOL	370	-21	2.5

3.3 Model Outputs

The simulation considers the retrofitting of an existing supercritical coal power plant installed in Gliwice, with a net power output of $900MW$. The hydrate capture system requires a total of $357.4MWel$ to function (39.7% of the plant net power output), that for a plant thermal efficiency of 45% corresponds to an energy penalty of 17.87%. Table 3.5 list the main outputs of the model. Considering an average cost for the THF of 2867€/ton[46], the annual expenditure to replenish the thermodynamic promoter is 26 M€. Thanks to ASPEN-Plus ICE (Integrated Cost Estimation), a first capital cost of the capture system can be extracted from the simulated process. Table 3.6 summarise the THF, capital and O&M (Operation And Maintainment) cost of the capture system based on ASPEN-Plus data-bank. A more accurate estimation is needed to assess the real costs of the implementation, especially for the high

Table 3.5: Model Output

Compressors power	MW	438
Pumps power	MW	8.6
Cooling power	MW	369.1
Turbine power	MW	-458.4
Total required power	MW	357.4
Captured CO_2	kg/s	155.2
CO_2 in exhaust gas	kg/s	15.5
Energy consumption/CO_2 produced	$MWh/ton CO_2$	0.64
CO_2 emission/Energy produced	$ton CO_2/MWh$	0.103
Make-up water[a]	kg/s	326.5
Make-up THF[b]	kg/s	0.35
Cooling water	kg/s	4500
Ethylene-glycol solution(30%mol)[c]	kg/s	1850

[a]Part of the water that participate to the reaction needs to be re-injected to maintain the correct ratio [b]0.1% of the THF is considered to remain in the hydrate flow stream and gets lost during the CO_2 recovery due to its volatility [c]This is a closed cooling cycle.

Table 3.6: Initial cost estimation

Total Capital Cost [$M€$]	306
Total Operating Cost [$M€/y$]	152.3
THF Cost [$M€/y$]	26

O&M and THF values.

Chapter 4

Post-combustion amine-based CO_2 absorption

This chapter describes more in detail the amine absorption process, reporting outputs from the analysis done by Krzysztof Bochon and Tadeusz Chmielniak[41], adopting the same data set used for the hydrate-based simulation for a comparison of the two methods.

4.1 Amine-based absorption

As mentioned in section 2.1, due mainly to the commercial deployment and development of the technology in the industrial sector and due to the chance of virtually retrofit any existing power plant, the choice of this comparison is between the post-combustion amine based absorption and hydrate-based separation of CO_2 from flue gas.

4.1.1 Choice of the sorbent

The post-combustion capture process is complicated by the low CO_2 partial pressure and the presence of other components in the gas stream. For these reasons, several different amine-based solvents have been studied to achieve energy efficient separations. In order to maximise these systems separation efficiency, the sorbent must respect several key aspects:

- High load of CO_2/sorbent unit volume;
- Low heat of desorption (it reduces the energy penalty for sorbent regeneration);
- Sorbent tolerance to contaminants (it reduces degradation and formation of by-products)
- Low sorbent costs.

Operate with high CO_2 loading can, from one side, inhibit solvent degradation by avoiding the formation of heat stable salts (interaction with SO_2) but on the other hand it has a first order effect on increasing the

degradation rate. High CO_2 loading also accelerate corrosion rates in amine plants[6]. Although several sorbents and sorbent mixtures are currently being tested, monoetanolamine (MEA, $CH_2CH_2OH-NH_2$) based sorbents are the most studied and commonly used, backed up by proven and readily available technology. For these reasons and due to the amount of data available, MEA is the choice for this comparison; MEA-based solvents are also rather economic. MEA and MDEA blends, when mixed at the appropriate ratio, are a good solvent choice because they combine the fast MEA-CO_2 reaction rate with MDEA higher absorption capacity and lower regeneration energy requirement. Alternatives to MEA-based solvents might have higher CO_2 capacity and lower energy consumption, however, just like sterically hindered amines (KS-1, KS-2 and KS-3),they have higher costs[47].

4.1.2 Limitations of the MEA process

Although MEA-based processes for CO_2 absorption from flue gas are technologically developed and commercially implemented, drawbacks like energy penalty, sorbent loss and corrosion are presents.

Energy penalty One of the major issues, as previously mention, is the energy penalty faced due to the large amount of heat required to break carbamate bonds and regenerate the sorbent. The drying and compression of the captured CO_2 for transport and storage also adds to the energy penalty[9]. This translates in the net efficiency reduction of the power plant, which implies the need of a higher capacity power plant to achieve the same net power generation achieved without CCS.

Sorbent loss Sorbent is partially lost during the process because of several reasons like solvent vaporisation or solvent degradation. Impurities like O_2, SO_2 and NO_2 react with MEA and form heat stable salts that reduce the sorbent absorption capacity. These salts can be treated in a sorbent reclaimer and some of the MEA can be retrieved, although this process adds to the plant energy penalties. Not all the MEA entering the stripper gets regenerated[48].

Corrosion This is a process treating oxygen-containing gases, therefore it is imperative to reduce corrosion rates. Maintaining adequate operation conditions together with the use of corrosion inhibitors and appropriate construction materials, helps addressing this issue[48].

Transport and disposal Once captured, CO_2 needs to be securely transported and stored in the appropriate sequestration site. While storage costs might be low, considering the treatment of thousands of CO_2 tonnes per day, pipelines appears to be the optimal transportation method. Construction of new pipelines or retrofitting of old installations might be not economically feasible, therefore transport via tankers is also considered. If used as a by-product for EOR (Enhanced Oil Recovery) or ECBM (Enhanced Coal Bed Methane) processes, CO_2 sequestration might generate revenues[48].

[9] As for the hydrate system, the compression energy for transport was not taken into account.

4.2 Process Description

A brief description on the post-combustion, MEA-based absorption, flue gas treatment for CO_2 capture will be given in this section. Figure 4.1 shows the related flow scheme. This is a continuous scrubbing system built around two main elements: an absorber (ABSORBER) for CO_2 absorption and a regenerator (STRIPPER) for sorbent recovery and release of CO_2 in concentrated form. Due to amine solvents

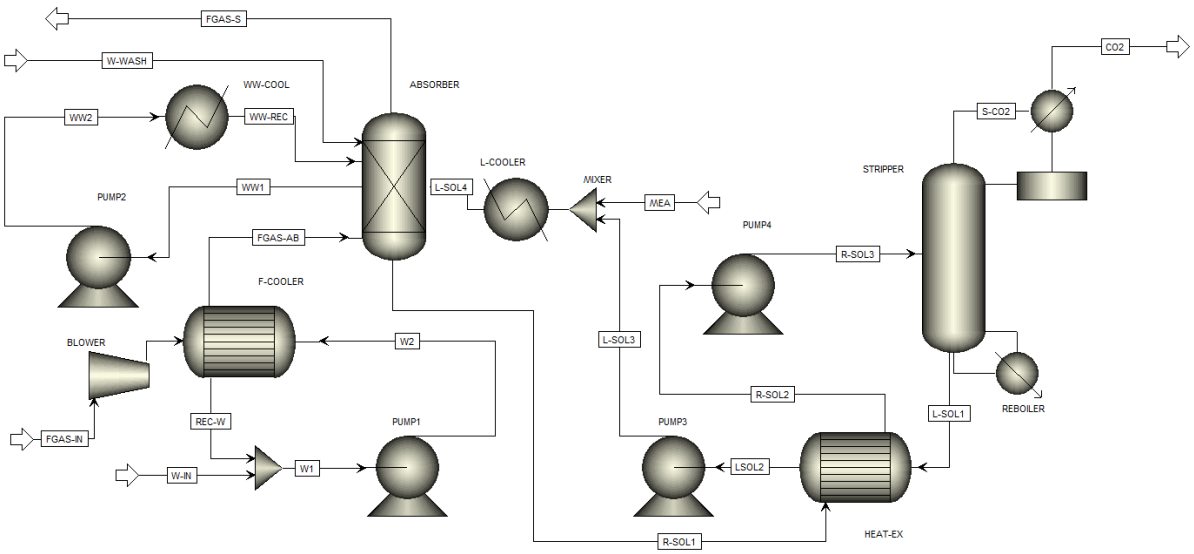

Figure 4.1: Process flow scheme for amine-based CO_2 capture from flue gas
Draw following Stephen A. Rackley scheme, Carbon Capture and Storage (Second Edition)[6]

low tolerance to NO_2 and SO_2 in the flue gas, the process requires the removal of these components ahead of the absorption. These removal processes will not be included in the analysis and the low residual NO_2 and SO_2 content is considered to not influence the separation process. Before entering the absorber tower (FGAS-AB in ABSORBER), the flue gas is pressurised (BLOWER) and cooled to 40 - 60 ℃ at atmospheric pressure (F-COOLER). Generally, the cooling choice falls onto direct water contact which works also as fine particulate matter remover. The lean solvent (low content of CO_2) enters the absorber tower (L-SOL4) and gets in contact with the flue gas (counter-current). The separation process uses amines that act like bases, they neutralise acid molecules like CO_2 by forming a weekly bonded component and releasing heat. The energy released using MEA as sorbent is approximately 3.5 $MJ/kg$$CO_2$. To avoid entrainment and transport of vapour and solvents droplets, flue gas is water washed (W-WASH) before it is vented to the atmosphere from the top of the tower (FGAS-S). The rich solvent (high content of CO_2) exits from the base of the tower (R-SOL1) and is heated (HEAT-EX) thanks to the heat recovered from the regenerated solvent cycling back into the stripping tower (STRIPPER). Afterwards, the rich solvent is pumped towards the stripping tower that operates at 100 – 140 ℃ and at slightly higher pressure than the absorber. A stream of steam and CO_2 exits the top of the stripping tower (S-CO2) and the steam is condensed to obtain a pure CO_2 product stream. The regenerated solvent is cooled (HEAT-EX + L-COOLER) and cycled back to the absorber tower. The reboiler supplies the heat required to reverse the absorption reaction. Fresh solvent is added to make up for losses in the process[6].

4.2.1 Equipment Analysis

This section describes the plant equipment shown in figure 4.1. The separation system consists of the following equipment:

F-COOLER A first heat exchanger is needed to cool the flue gases coming out of a power plant. The initial flue gas temperature can range between 60 and 550 °C or more, in dependence if treating coal-fired power plants (with wet SO_2 scrubbers) or natural gas-fired power plants. In order to improve the absorption efficiency, minimize sorbent losses and avoid excessive loss of moisture with the exhaust gases, FGAS-AB temperature is set to 45-50 °C with the FGAS-IN temperature of 60 °C.

PUMP1-2-3 Whether it is for water, lean or rich solvent, a set of pumps is needed to overcome the respective pressure drops.

BLOWER The flue gas is pressurised to overcome a substantial pressure drop occurring when it passes through the absorber tower.

ABSORBER The reaction between CO_2 and the MEA sorbent occurs in this vessel. The ABSORBER, in which the CO_2 gets dissolved in the sorbent, functions in counter-current. The majority of the absorbers are designed as polymer-based packed columns with large inter-facial area but plate-type applications are also a viable option.

HEAT-EX Before the CO_2 rich sorbent can be regenerated and stripped off the CO_2 it needs to be heated while, at the same time, the lean sorbent coming out of the STRIPPER needs to be cooled before it can be circulated back to the ABSORBER. HEAT-EX is a cross heat exchanger in which these two sorbent streams pass through and get heated (rich sorbent) and cooled (lean sorbent).

L-COOLER Another cooler (L-COOLER) is necessary to bring back the lean solvent to an acceptable temperature (40 °C) before recirculating it into the absorber column.

MIXER A small amount of fresh MEA has to be added to the sorbent stream to make up for sorbent losses.

STRIPPER This is the regeneration tower where CO_2 gets separated from the sorbent with the application of heat. It operates between 100 and 140 °C and at a pressure slightly higher than the absorber tower. CO_2 is then separated in a flash separator to obtain an almost pure CO_2 stream.

REBOILER This is a heat exchanger in which low-pressure steam is used to heat the rich sorbent coming from the STRIPPER bottom feed, providing the needed energy for CO_2 separation and solvent regeneration.

4.3 Outputs

The outputs of this analysis are based on the publication of Krzysztof Bochon and Tadeusz Chmielniak on Energy analysis of the carbon dioxide capture installation with the use of monoethanolamine[41]. For obvious reasons, the data of flue gas flow-rate and composition, based on the supercritical power plant with net power output of the $900MW$, are the same as the ones used to design the hydrate-based process in chapter 3. The amine capture system requires a capture heat duty of $550.2MW$. The heat power comes directly from the power plant steam generation cycle, therefore considering a thermal efficiency of 45%, $1400MW$ remain available for electricity production. Considering also the $86MW$ needed by coolers and compressors, the energy penalty for this specific scenario is of 16.68%, cutting 37% of the plant net power output. Table 4.1 shows the output of the amine based process. From a

Table 4.1: Power and energy needs

Flue gas mass flow	kg/s	824.2
Captured CO_2	kg/s	157.4
CO_2 in exhaust gas	kg/s	17.5
Capture degree	%	90
Capture heat duty	MW	550.2
Heat demand ratio for capture	$MJ/kgCO_2$	3.49
CO_2 emission/Energy produced	$tonCO_2/MWh$	0.111
Power of compressors and coolers	MW	86.0
Energy consumption/CO_2 produced	$MWh/tonCO_2$	0.59

Reproduced from K. Bochon and T. Chmielniak, Energy and economic analysis of the carbon dioxide capture installation with the use of monoethanolamine and ammonia[41]

quick comparison of the two treatment systems outputs it is noticeable that, with 0.64 $MWh/tonCO_2$, the hydrate-based capture system requires more energy than the MEA-based one (0.59 $MWh/tonCO_2$). Nevertheless, the power plant equipped with the hydrate system would emit less CO_2 per MWh than the same plant equipped with the MEA system in exam : 0.103 $tonCO_2/MWh$ for the clathrate capture while 0.111 $tonCO_2/MWh$ for the MEA absorption[10]. The next chapter analyses the results and proceed with a more detailed comparison.

[10]These last two values may differ because of calculation approximations.

Chapter 5

Results

This chapter summarises the results obtained from the simulations in terms of power plant energy penalty and electricity market profits.

5.1 Energy and cost Comparison

The comparison of the two separation methods, hydrate and MEA-based, considers the retrofitting of an existing supercritical coal power plant installed in Gliwice with a net power output of $900MW$. The hydrate capture system requires a total of $357.4MWel$ to function, while $333.6MWel$ are needed for the MEA system, cutting off 39.7% and 37% of the plant net power output respectively. For a thermal efficiency of 45%, these values correspond, respectively, to an energy penalty of 17.87% and 16.68%, which means lowering the power plant efficiency to 27% with the hydrate system implementation and 28% through the use of the MEA system analysed. Table 5.1 summarises the energy comparison main outcomes. A non extensive, initial economic analysis was also performed: it takes into account only

Table 5.1: Energy comparison main outcomes

	Base plant	MEA separation	Hydrate separation
Capture system life [y]	25		
Working hours [h/y]	7200		
Net Power output [MW]	900	566.4	542.6
Plant efficiency [%]	45	28	27
Energy penalty [%]	0	16.68	17.87
Electricity produced [GWh/y]	6480	4078.15	3907.04

the hydrate capture system, excluding the power plant fuel, O&M and income taxes costs. The life expectancy of the capture system is set to 25 years, working alongside the power plants for 7200 h/y. The analysis is based on the average European electricity market price (50 €$/MWh$[49]) and carbon

price (12.78 €/$ton$$CO_2$[50]). Referring solely to the profits obtained through the electricity market, by maintaining constant both electricity and carbon price, the implementation of the hydrate system lowers the annual net electricity income of the power plant by 28.51% while the MEA process reduces it of the 25.54%. Table 5.2 summarises the basic cost outputs. It is clear that the implementation of one of these

Table 5.2: Basic cost comparison outputs considering fixed carbon and electricity market prices

	Base plant	MEA separation	Hydrate separation
Electricity produced [GWh/y]	6480	4078.15	3907.04
Electricity market price [€/MWh][a]	50		
Net electricity income [$M€/year$]	324	203.9	195.4
CO_2 produced [$Mton/y$]	4.5	0.5	0.4
CO_2 captured [$Mton/y$]	0	4.1	4.0
CO_2 emission/Energy production [$tonCO_2/MWh$]	0.7	0.111	0.103
Cost of CO_2 production [€/$ton$$CO_2$]	0	29.44[c]	32[c]
Carbon price[b] [€/$ton$$CO_2$]	12.78		
CO_2 cost [$M€/y$]	57.9	5.8	5.1
Profit [$M€/y$]	266.1	198.1	190.2

[a]Average value reported on the quarterly report on European electricity markets 2018 by the EU Commission[49] [b]Due to a great difference with the la quarter of 2017 and the present day, the value was updated at the 07-05-2018[50] [c]Value in line with the Global CCS Institute[51]

capture systems greatly cuts the CO_2 emission (up to 91%), lowering the carbon footprint by 4 - 4.1 Mton/y. These great savings come with a price: installation, O&M and THF costs lower noticeably the net electricity income. As shown in section 3.3, a first estimation on capital and O&M costs is obtained through the simulator, which outputs a total capital cost of 306 M€ and a total O&M cost of 152.3 M€/y. Considering the THF price of 2867 €/ton[46], due to the loss of 0.1%/s (weight fraction), and added cost of 26 M€/y was added to the O&M costs (table 5.3). At the current average market price of 50€/MWh,

Table 5.3: Hydrate separation system costs

	Hydrate separation
Total Capital Cost [M€]	306
Total Operating Cost [M€/y]	178.3

considering solely profits obtained from the electricity sale, the hydrate system implementation results to be not economically feasible. This is mainly due to the high O&M costs of the separation system and the chosen average market price for electricity. In order to pay back for the separation system within its life expectancy, with a discount rate of 15%, a minimum price of 59.08 €/MWh must be adopted (see figure 5.1). This value was obtained through a sensitivity analysis over the net present value (NPV) calculated

with the equation 5.1.

$$NPV = Capital\ costs + \sum_{t} \frac{Revenues - O\&M\ costs}{(1+i)^t} \tag{5.1}$$

Where

$i =$ Discount rate

$t =$ Cash flow time

If one of the higher electricity price were to be considered, (62 €/MWh for example[49]), the pay-

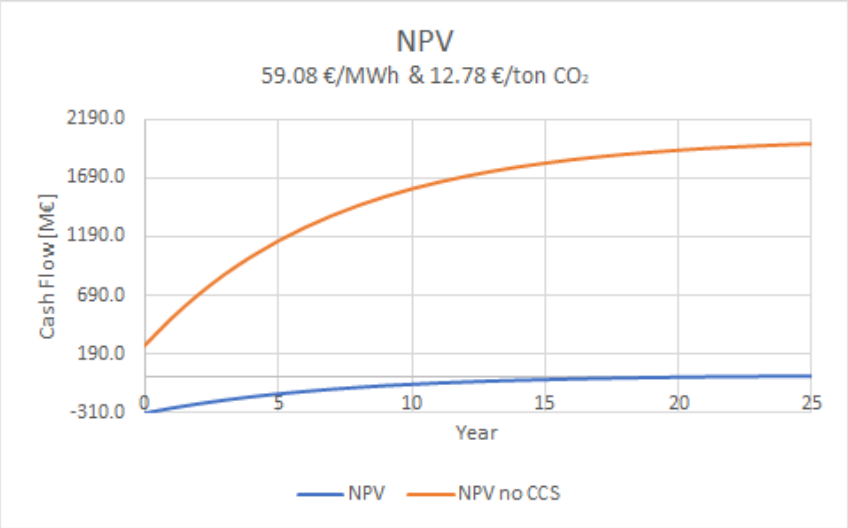

Figure 5.1: NPV chart with a payback period of 25 years

back period for the capture system would be of ∼10 years (see figure 5.2). Maintaining the same annual

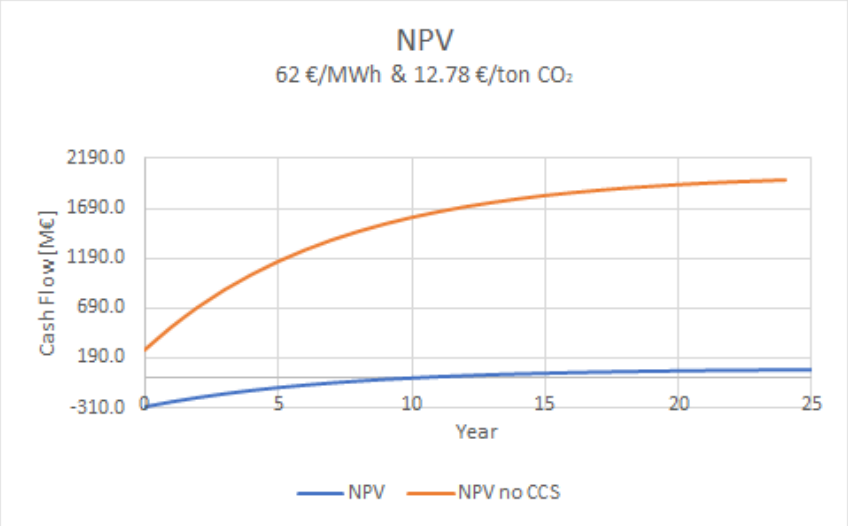

Figure 5.2: NPV chart with a payback period of 10 years

profit as the power plant without a CCS installation, considering solely the electricity sale and keeping all

the other parameters constants, would require for the electricity price to raise to 69.42 €/MWh[11]. In this case, as shown in figure 5.3, the payback period will go down to ∼5 years. Beside the high O&M cost

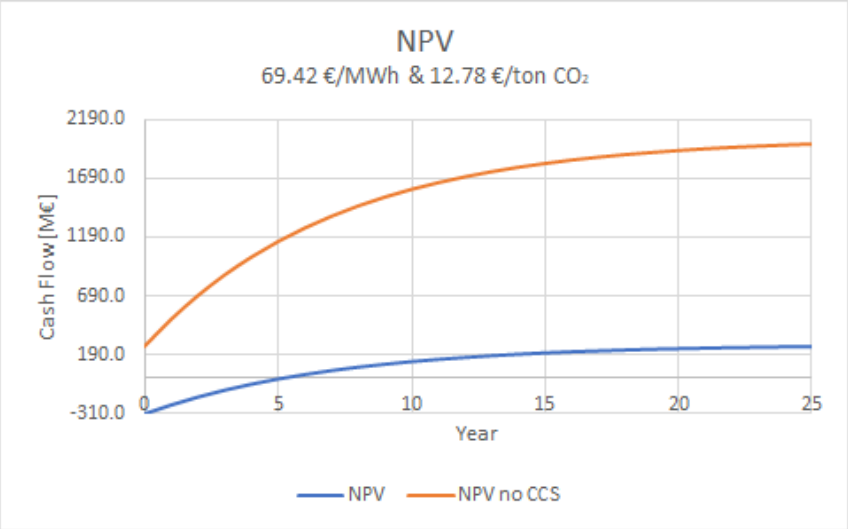

Figure 5.3: NPV chart with a payback period of 5 years

of the CCS system, the low carbon price of 12.78 €/ton of CO_2 plays a crucial role in the system feasibility evaluation. Another sensitivity analysis shows that, with an electricity market price of 62 €/MWh, increasing the carbon price to 36.62 €/tonCO_2, would levelise the profits as shown in table 5.4. In this

Table 5.4: Alternative scenario cost outputs

	Base plant	Hydrate separation
Electricity market price [€/MWh][a]	62	
Carbon price [€/tonCO_2][a]	36.62	
Electricity produced [GWh/y]	6480	3907.04
CO_2 produced [Mton/y]	4.5	0.4
CO_2 cost [M€/y]	175.1	15.5
Profit [M€/year]	226.7	

[a]All the other factors as constants,

case, the payback period would be of ∼21 years, as shown in figure 5.4. In all the mentioned scenarios, even though a positive NPV is achievable, the profit over 25 years is noticeably lower when compared to the profit obtainable by the power plant without a CCS system. It is important to notice that no O&M cost for the power plant without CCS were considered, therefore its profit should be lower than the calculated one. If CO_2 sales were to be considered at the same constant average market price of electricity and CO_2, the investment outcome might positively change in economic terms. Due to the market CO_2 need trends, the calculations were carried on considering the total sale of the 4 $Mton$ of CO_2 produced, keeping an average fixed sale price of 5€/$ton$$CO_2$[51] over the years, at the same discount rate. Figure

[11]This price assumption is reasonable considering the market trend reported by the EU Commission[49]

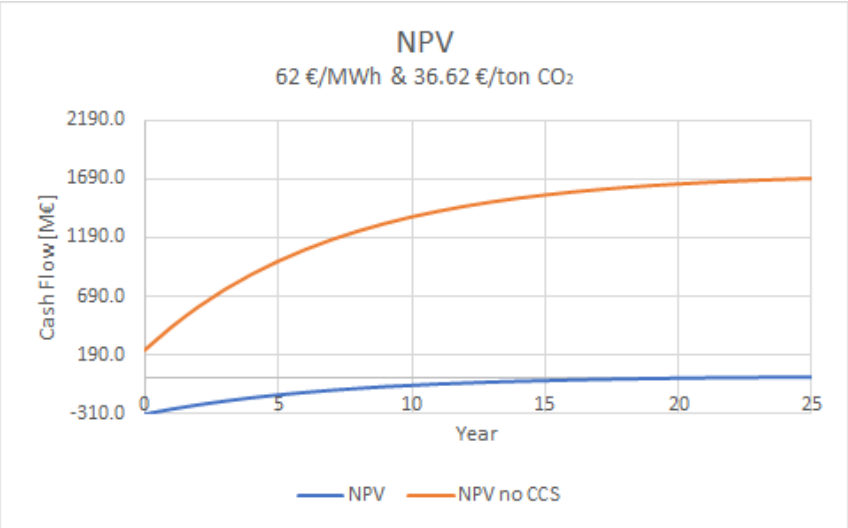

Figure 5.4: NPV chart with a payback period of 21 years

5.5 shows the resulting NPV. In this case scenario, despite the conservative approximations, the capture system looks profitable. According to recent reports, the energy market proceeds towards a lowering of

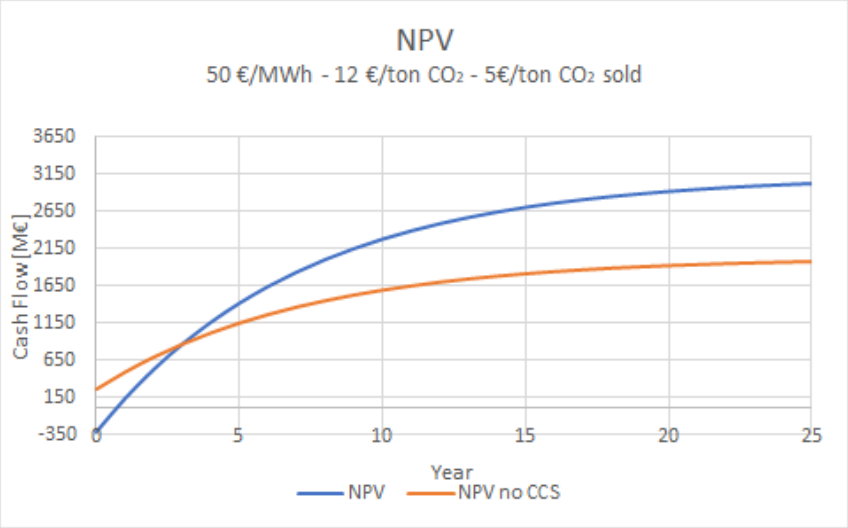

Figure 5.5: NPV chart in case of CO_2 sales at 5€$/ton$

the current energy prices while the cost of CO_2 emitted will increase[12]. On these terms, although the overall profit will be lower, the capture process might become economically feasible and a must in order to keep fossil fuels plant running with a certain profit margin. Further work is needed to assess this possibility.

[12]The assumed EU market price for the year 2018 of 8.2 €/ton was already surpassed on February 2018[49][50]

Chapter 6

Conclusions

This work mainly compared two CO_2 separation technologies, MEA-based absorption and THF-hydrate capture. The choice of this specific comparison was mainly based on data availability and reliability, therefore these outcomes may not fully apply to other models. Applying either one of these two technology to an existing 900 MWel power plant requires a great amount of power, but between the two there is not a large difference in terms of energy penalty (16.68% for MEA absorption, 17.87% for THF-hydrate capture). If no monetary income streams related to the CO_2 sale is taken into account, at the current techno-economic conditions, the obtained results deem CO_2 capture systems unprofitable. At the current CO_2 and EU electricity average market price (12.78 €/tonCO_2 and 50 €/MWhel), the analysed separation technologies greatly lower the electricity sale profits (28.51% less for hydrates, 25.54% less for MEA) when compared to the power plant without CCS implementation. In order to change this situation, government support is essential, not only at the investment stage but also in defining a more appropriate carbon price and adopting an effective green certificate regulation system. For the analysed technology, a great amount of CO_2 emissions can be avoided: more than 4 MtonCO_2 can be captured, stored, sold or reused every year. Thus, considering selling the captured CO_2 at a fixed price of 5€$/ton$$CO_2$, at the current CO_2 and EU electricity average market price, the calculated income positively changes turning the modelled capture system profitable. Still, research on CO_2 capture through hydrates, aiming not only at power plants but also at other sectors for future commercialisation, is mainly done through computer simulation. This is a huge disadvantage if compared with the possibility to test other technologies in pilot and plant scale: despite the numerous advantages and potential of clathrates, gas absorption remains the most promising solution for CO_2 recovery because it is an industrially developed technology, implemented in other gas treatment processes and easily adaptable to CO_2 capture. With the proper solvent choice (a different MEA blend, for example) and system optimisation, greater energy savings could be achieved. Nevertheless, all the results are in accordance with theory and scientific literature, which allows to say that hydrate separation is a promising technology that deserve more in-detail analysis and field tests.

6.1 Future Work

There are several areas of improvement that should be addressed to obtain more accurate outputs. This section proposes few ideas to be implemented in future works.

- ASPEN-Plus is a great tool for process and energy engineering. Thanks to its extensive data-bank it is the optimal choice for chemical reactions and energy-integration operations, but it is not optimised for hydrate formation reactions, therefore the adoption of another ad-hoc software is advised.
- In order to effectively simulate the capture process and obtain reliable energy and costs results, proper parameters were assigned to each equipment follow engineering manuals. Nevertheless, a focus on the plant equipment dimensioning is necessary to obtain more concrete and optimised results.
- Energy consumption could be reduce by integrating the power generation plant in the simulation of the CO_2 capture system.
- Another way to greatly reduce the energy consumption is to analyse the implementation of a reactor start-up process before getting into the steady state of flue gas treatment. The initial hydrate crystals formation allows for clathrates nucleation at higher temperatures and lower pressures.
- LCOE and LCA analysis are needed to obtain a more accurate assessment.

Bibliography

[1] NORA. Trends in atmospheric carbon dioxide. Data, National Oceanic and Atmospheric Administration Earth System Research Laboratory, Global monitoring division, 2018.

[2] IPCC. Climate change 2014: Synthesis report. Report 5, Intergovernmental Panel on Climate Change, 2014. Contribution of Working Groups I, II and III to the Fifth Assessment Report of the Intergovernmental Panel on Climate Change [Core Writing Team, R.K. Pachauri and L.A. Meyer (eds.)]. IPCC, Geneva, Switzerland, 151 pp.

[3] IEA. CO_2 emissions from fuel combustion highlights. Report, International Energy Agency, 2016.

[4] IEA. Carbon capture and storage: The solution for deep emissions reductions. Publication, International Energy Agency, 2015.

[5] Filip Neele Eliane Blomena, Chris Hendriksa. Capture technologies: Improvements and promising developments. Report 1505-1512, ECOFYS, TNO, 2009.

[6] Stephen A. Rackley. Carbon capture from power generation. In Elsevier Inc, editor, *Carbon Capture and Storage (Second Edition)*. Butterworth-Heinemann, 2017.

[7] M. Mercedes Maroto-Valer Dennis Y.C. Leung, Giorgio Caramanna. An overview of current status of carbon dioxide capture and storage technologiess. Publication, Department of Mechanical Engineering: The University of Hong Kong, Hong Kong; Centre for Innovation in Carbon Capture and Storage: Heriot-Watt University, UK, 2014.

[8] Erik Meuleman et. all. CO_2 capture performance of mea and blended amine solvents in csiro's pilot plant with flue gas from a brown coal-fired power station. Publication, CSIRO Energy Technology, Clayton, VIC, Australia, 2010.

[9] Nathan A. Hatcher Ralph H. Weiland. Post-combustion CO_2 capture with amino-acid salts. Publication, Optimized Gas Treating, Inc., 2011.

[10] Selen Cremaschi Aroonsri Nuchitprasittichai. Optimization of CO_2 capture process with aqueous amines using response surface methodology. Publication, Department of Chemical Engineering, The University of Tulsa, USA, 2011.

[11] Maohong Fan Bryce Dutcher and Armistead G. Russel. Amine-based CO_2 capture technology development from the beginning of 2013 - review. Publication, Department of Chemical and Petroleum

Engineering, University of Wyoming, USA - School of Civil and Environmental Engineering, Georgia Institute of Technology, Atlanta, Georgia, USA, 2015.

[12] M. Wang et all. Post-combustion CO_2 capture with chemical absorption: A state-of-the-art review. Publication, Process Systems Engineering Group, School of Engineering, Cranfield University, Uk - RWE npower, Windmill Hill Business Park, UK, 2011.

[13] M.M. Maroto-Valer M. Olivares-Marín. Preparation of a highly microporous carbon from a carpet material and its application as CO_2 sorbent. Publication, Centre for Innovation in Carbon Capture and Storage (CICCS), Energy and Sustainability Research Division, Faculty of Engineering, University of Nottingham, University Park, Nottingham, Uk, 2011.

[14] M.M. Maroto-Valer M. Olivares-Marín. Development of adsorbents for CO_2 capture from waste materials: a review. Publication, University of Extremadura, Badajoz, Spain; CICCS, University of Nottingham, UK, 2012.

[15] Jitae Kim Thi-Huong Pham, Byeong-Kyu Lee. Novel improvement of CO_2 adsorption capacity and selectivity by ethylenediamine-modified nano zeolite. Publication, Department of Civil and Environmental Engineering, University of Ulsan, Daehakro R93, Nam-gu, Ulsan 680-749, Republic of Korea, 2016.

[16] Olav Bolland Luca Riboldia. Overview on pressure swing adsorption (psa) as CO_2 capture technology: state-of-the-art, limits and potentials. Publication, Energy and Process Engineering Departament, the Norwegian University of Science and Technology, Norway, 2017.

[17] David S. Sholl Ambarish R. Kulkarni. Analysis of equilibrium-based tsa processes for direct capture of CO_2 from air. Publication, School of Chemical and Biomolecular Engineering, Georgia Institute of Technology, Atlanta, United States, 2012.

[18] Shuaifei Zhao et. all. Status and progress of membrane contactors in post-combustion carbon capture: A state-of-the-art review of new developments. Publication, Department of Environmental Sciences - Macquarie University and CSIRO Energy, Australia. Department of Chemical Engineering - Norwegian University of Science and Technology, Norway. LRGP-CNRS Université de Lorraine and Université Claude Bernard de Lyon, France. College of Engineering - Huazhong Agricultural University,China. UNESCO Centre for Membrane Science and Technology - School of Chemical Engineering - The University of New South Wales, Australia. Membrane Science and Technology Research Centre - Nanjing Tech University, China, 2016.

[19] Edward S. Rubin Haibo Zhai. Techno-economic assessment of polymer membrane systems for postcombustion carbon capture at coal-fired power plants. Publication, Department of Engineering and Public Policy, Carnegie Mellon University, Pittsburgh, United States, 2013.

[20] Ming Zhao Guozhao Ji. Membrane separation technology in carbon capture. In *Recent Advances in Carbon Capture and Storage*. INTECH, 2017.

[21] G. Barbieri A. Brunetti, F. Scuraa and E. Drioli. Membrane technologies for CO_2 separation. Publication, National Research Council, Institute for Membrane Technology (ITM–CNR) and Department of Chemical Engineering and Materials, Via Pietro BUCCI, 87030 Rende CS, Italy, 2009.

[22] Nikolay N. Akinfiev Larryn W. Diamond. Solubility of CO_2 in water from -1.5 to 100℃ and from 0.1 to 100 mpa: Evaluation of literature data and thermodynamic modelling. Publication, Institute of Geological Sciences, University of Bern, Baltzerstrasse, Switzerland, 2003.

[23] Caineng Zou. Cryogenic and distillation systems. In Elsevier Inc, editor, *Unconventional Petroleum Geology (Second Edition)*. Johnathan Simpson, 2017.

[24] Jose´ D. Figueroa et. all. Advances in CO_2 capture technology—the u.s. department of energy's carbon sequestration program. Publication, National Energy Technology Laboratory, U.S. Department of Energy and Science Applications International Corporation, National Energy Technology Laboratory, Pittsburgh, United States, 2008.

[25] Marta E. Torres Gerhard Bohrmann. Gas hydrates in marine sediments. In Matthias Zabel Horst D. Schulz, editor, *Marine Geochemistry*. Springer, 2006.

[26] Carolyn Koh E. Dendy Sloan. Gas hydrates in marine sediments. In Taylor and Francis Group, editors, *Clathrate Hydrates of Natural Gases, Third Edition*. CRC Press, 2008.

[27] Junnan He et. all. A literature research on the performance evaluation of hydrate-based CO_2 capture and separation process. Publication, Key Laboratory of Efficient Utilization of Low and Medium Grade Energy (Tianjin University), Ministry of Education of China, China - Sir Joseph Swan Centre of Energy Research, Newcastle University, UK, 2017.

[28] Jianfeng Tang et. all. Study on the influence of sds and thf on hydrate-based gas separation performance. Publication, Natural Gas Hydrate Laboratory, College of Pipeline and Civil Engineering, China University of Petroleum (East China), Shandong - PetroChina Coalbed Methane Co., Beijing - West-East Gas Transmission Company Pipeline Branch, Shanghai, China, 2013.

[29] Peter Englezos Praveen Linga, Adebola Adeyemo. Medium-pressure clathrate hydrate/membrane hybrid process for postcombustion capture of carbon dioxide. Publication, Department of Chemical and Biological Engineering, University of British Columbia, Vancouver, Canada, 2007.

[30] Jean-Michel Herri Nguyen Hong Duc, Fabien Chauvy. CO_2 capture by hydrate crystallization – a potential solution for gas emission of stee lmaking industry. Publication, Centre SPIN, Ecole Nationale Supe´rieure des Mines de St-Etienne, Saint-Etienne Cedex 2, France, 2007.

[31] Xuemei Lang Shuanshi Fan, Yanhong Wang. CO_2 capture in form of clathrate hydrate - problem and practice. Publication, School of chemistry and chemical engineering, Key Lab of Enhanced Heat Transfer and Energy Conservation, Ministry of Education, South China University of Technology, Guangzhou, China, 2011.

[32] Fumio Kiyono Hideo Tajima, Akihiro Yamasaki. Energy consumption estimation for greenhouse gas separation processes by clathrate hydrate formation. Publication, National Institute of Advanced Industrial Science and Technology, Tsukuba, Japan, 2004.

[33] Chunfeng Song et. all. Advanced cryogenic CO_2 capture process based on stirling coolers by heat integration. Publication, Tianjin Key Laboratory of Indoor Air Environmental Quality Control and Key Laboratory of Efficient Utilization of Low and Medium Grade Energy - School of Environmental Science and Technology - Tianjin University, China. Graduate School of Life and Environmental Sciences, University of Tsukuba, Japan, 2017.

[34] D. Keith Roper J. D. Seader, Ernest J. Henley. Kinetics and mass transfer. In Jennifer Welter, editor, *Separation Process Principles, Chemical and Biochemical Operations (Third Edition)*. John Wiley and Sons, Inc., 2011.

[35] Paulo L.C. Lage Cláudio P. Ribeiro Jr. Modelling of hydrate formation kinetics: State-of-the-art and future directions. Publication, Programa de Engenharia Química-COPPE, Universidade Federal do Rio de Janeiro, Rio de Janeiro, Brazil, 2008.

[36] P. R. Bishnoj V. Natarajan and N. Kalogerakis. Induction phenomena in gas hydrate nucleation. Publication, Department of Chemical and Petroleum Engineering, University of Calgary, Calgary, Alberta, Canada, 1994.

[37] Sebastien Bergeron and Phillip Servio. Reaction rate constant of CO_2 hydrate formation and verification of old premises pertaining to hydrate growth kinetics. Publication, Dept. of Chemical Engineering, McGill University, Montreal, Canada, 2008.

[38] H. Renon and J.M. Prausnitz. Local compositions in thermodynamic excess functions for liquid mixtures. Publication, University of California, Berkeley, California, 1968.

[39] Otto Redlich and J.N.S. Kwong. On the thermodynamics of solutions v. an equation-of-state. fugacities of gaseous solutions. Publication, Shell Development Company, Emeryville, California, 1948.

[40] Fatma Elif Genceli G uner. Feasibility study of $MgSO_4$ hydrate production by eutectic CO_2 clathrate crystallization. Publication, Chemical Engineering Department, Istanbul Technical University, Istanbul, Turkey - Intensified Reaction and Separation Systems Section, Process and Energy Department, Delft University of Technology, Delft, The Netherlands, 2015.

[41] Tadeusz Chmielniak Krzysztof Bochon. Energy and economic analysis of the carbon dioxide capture installation with the use of monoethanolamine and ammonia. Publication, Silesian University of Technology, Institute of Power Engineering and Turbomachinery, Gliwice, Poland, 2015.

[42] Fernando L. P. Pessoa Cláudia F. S. Lirioa. Enthalpy of dissociation of simple and mixed carbon dioxide clathrate hydrate. Publication, IFRJ - Paracambi and UFRJ- Escola de Química, Paracambi, RJ. Brasil, 2013.

[43] Adebola Adeyemo Praveen Linga and Peter Englezos. Medium-pressure clathrate hydrate/membrane hybrid process for postcombustion capture of carbon dioxide. Publication, Department of Chemical and Biological Engineering, University of British Columbia, Vancouver, Canada, 2007.

[44] Fumio Kiyono Hideo Tajima, Akihiro Yamasaki. Energy consumption estimation for greenhouse gas separation processes by clathrate hydrate formation. Publication, National Institute of Advanced Industrial Science and Technology, Onogawa, Japan, 2003.

[45] Carl R. Branan. -. In Elsevier, editor, *Rules of thumb for chemical engineers - A manual of quick, accurate solutions to everyday process engineering problems (Fourth Edition)*. Gulf Professional, 2005.

[46] *ICS Indicative Chemical Prices*. https://www.icis.com/chemicals/channel-info-chemicals-a-z/.

[47] M. Wang, J. Sidders A. Lawal, P. Stephensonb, and C. Ramshaw. Post-combustion CO_2 capture with chemical absorption: A state-of-the-art review. Publication, Process Systems Engineering Group, School of Engineering, Cranfield University and RWE npower, Windmill Hill Business Park, UK, 2011.

[48] Anand B. Rao. Details of a technical, economic and environmental assessment of amine-based CO_2 capture technology for power plant greenhouse gas control. Publication, Carnegie Mellon University Center for Energy and Environmental Studies, Pittsburgh, US, 2002.

[49] Market Observatory for Energy of the European Commission. Quarterly report on european electricity markets. Publication, European Commission, Directorate-General for Energy, Market Observatory for Energy, 2018, 2018.

[50] Markets Insider. CO_2 european emission allowances. http://markets.businessinsider.com/commodities/co2-emissionsrechte/euro, May 2018.

[51] Global CCS Institute. The CO_2 market. https://hub.globalccsinstitute.com/publications/accelerating-uptake-ccs-industrial-use-captured-carbon-dioxide/2-co2-market.

Appendix A

Appendix A